Available online at www.sciencedirect.com
SCIENCE DIRECT®
Tectonophysics 381 (2004) 29–59
TECTONOPHYSICS
www.elsevier.com/locate/tecto

Lithosphere structure of the Ukrainian Shield and Pripyat Trough in the region of EUROBRIDGE-97 (Ukraine and Belarus) from gravity modelling

T.P. Yegorova[a,*], V.I. Starostenko[a], V.G. Kozlenko[a], J. Yliniemi[b]

[a] *Institute of Geophysics, National Academy of Sciences, Kiev, Ukraine*
[b] *Geophysical Observatory of University of Oulu, Oulu, Finland*

Received 8 May 2001; accepted 18 June 2002

Abstract

The southern segment of the seismic profile EUROBRIDGE—EUROBRIDGE-97 (EB'97)—located in Belarus and Ukraine, crosses the suture zone between two main segments of the East European Craton—Fennoscandia and Sarmatia—as well as Sarmatia itself. At the initial stage of our study, a 3-D density model has been constructed for the crust of the study region, including the major part of the Osnitsa–Mikashevichi Igneous Belt (OMIB) superimposed by sediments of the Pripyat Trough (PT), and three domains in the Ukrainian Shield—the Volhyn Domain (VD) with the anorthosite–rapakivi Korosten Pluton (KP), the Podolian Domain (PD), and the Ros–Tikich Domain (RTD). The model comprises three layers—sediments with maximum thickness (6 km) in the PT and two heterogeneous layers in the crystalline crust separated at a depth of 15 km. 3-D calculations show the main features of the observed gravity field are caused by density heterogeneities in the upper crust. Allocation of density domains deeper than 15 km is influenced by Moho topography. Fitting the densities here reveals an increase (up to 2960 kg m^{-3}) in the modelled bodies accompanied by a Moho deepening to 50 km. In contrast, a Moho uplift to a level of 35–37 km below the KP and major part of the PT is associated with domains of reduced densities. An important role for the deep Odessa–Gomel tectonic zone, dividing the crust into two regions one of basically Archean consolidation in the west (PD and RTD) and one of Proterozoic crust in the east (Kirovograd Domain)—was confirmed.

2-D density modelling on the EB'97 profile shows that in the upper crust three main domains of different Precambrian evolution—the OMIB (with the superimposed PT), the VD with the KP, and the PD—can be distinguished. Deeper, in the middle and lower crust, layered structures having no connection to the surface geology are dominant features of the models. Least thickness of the crust was obtained below the KP. Greatest crustal thickness (more than 50 km) was found below the PD, characterised also by maximum deviation of velocity/density relation in the rocks from a standard one. The velocity and density models along the EB'97 profile have been interpreted together with inferred V_p/V_s ratios to estimate crustal composition in terms of SiO_2 content. In the course of the modelling, the status of the PD as a centre of Archean granulitic consolidation has been confirmed. The crustal structure of the anorthosite–rapakivi KP is complex. For the first time, a complicated structure for the lower crust and lower crust–upper mantle transition zone beneath the KP has been determined. The peculiarities of the crustal structure of the KP are quite well explained in terms of formation of rapakivi–anorthosite massifs as originating from melt chambers in the upper mantle and lower crust. An important role for the South Pripyat Fault (SPF), repeatedly activated during Proterozoic–Palaeozoic times, has been ascertained. At the subplatform stage of crustal evolution the SPF was,

* Corresponding author.
E-mail address: egorova@igph.kiev.ua (T.P. Yegorova).

doi:10.1016/j.tecto.2002.06.003

probably, a magma channel facilitating the granitic intrusions of the KP. In the Palaeozoic the fault was reactivated during rifting in the PT.

Keywords: 3-D gravity modelling; Crustal structure and composition; Precambrian Ukrainian Shield; Pripyat Trough; Korosten Pluton; Rapakivi–anorthosite

1. Introduction

Seismic profile EUROBRIDGE links two Precambrian shields—Baltic and Ukrainian. Its southern segment, acquired in 1997, crosses, from north to south, a region of complex geological structure comprising the Osnitsa–Mikashevichi Igneous Belt (OMIB), with superimposed Pripyat Trough (PT), and the Ukrainian Shield (Fig. 1). Interpretation of seismic data along the profile together with available geological and geophysical information is here used for better understanding the structure, composition, and evolution of the Earth's crust of the region. Additional important information is gained from the results of gravity modelling. Before the processing of seismic data on EUROBRIDGE-97 (EB'97) profile for the study region, limited by 49–54° north and 26–34° east, we constructed a 3-D density model for the crust, summarising previously obtained geological and geophysical information in the region. This model was presented in the EUROPROBE Workshops (Suwalki, Poland, 1999; Tulcea, Romania, 1999; Gurzuf, Crimea, Ukraine, 2000). It was used for carrying out subsequent stages of work namely, 2-D gravity modelling along the EB'97 profile on the basis of seismic models along the profile. As a result, a density cross-section representing the main features of the Earth's crustal structure along with a prediction of the composition of its main layers has been constructed.

The study region for the 3-D density model is well-understood from the geological and geophysical points of view. The region is crossed by three DSS profiles surveyed and interpreted in the 1980s. Since that time, an active interpretation of the gravity and magnetic fields has been made, resulting in the construction of density models at various scales (from regional to local). Huge quantities of rock physical property measurements were made in laboratories; composition and age of geological formations have been studied thoroughly. However, systematic generalisation of the whole complex of geological and geophysical data was absent. This work was initiated by carrying out the seismic investigations on EB'97 profile; the development of a 3-D density model is considered to provide a framework, within which new data can be linked together with previously obtained data.

Fig. 1. Main tectonic units of the crystalline basement of the EUROBRIDGE-97 area. BBG—Belarus–Baltic Granulite Belt, BGM—Bragin Granulite Massif, CB—Central Belarus Belt, CH—Chernigov block of the Pripyat–Dnieper–Donets Basin (PDDB), DB—Dnieper Basin of the PDDB, EL—East Lithuanian–Latvian Belt, KD—Kirovograd Domain of the Ukrainian Shield (USh), KNP—Korsun–Novomirgorod pluton of the KD, KP—Korosten Pluton of the Volhyn Domain (VD), NV—Novograd–Volhyn block of the VD, OMIB—Osnitsa–Mikashevichi Igneous Belt, PD—Podolian Domain of the USh, PT—Pripyat Trough of the PDDB, RTD—Ros–Tikich Domain of the USh, VG—Vitebsk Granulite Domain. 1—Linear zones of tectonic activation and superimposed depressions; 2–4 volcanic and plutonic belts, 2—complex rapakivi–anorthosite massifs: rapakivi–anorthosites (a), rapakivi granites (b), anorthosites (c), gabbros (d); 3—layered massifs of basic rocks; 4—volcanic belts and superimposed troughs; 5—craton areas of widespread granitisation: granitic massifs (a) and granite–migmatite domains (b); 6—epicratonic troughs; 7—suture troughs and thrust zones; 8—deep suture zone Odessa–Gomel; 9—volcano-tectonic depressions; 10—amphibolite–gneiss belts—projections of metabasite–amphibolite basement and migmatite–plagiogranite domains; 11–13 granulite belts: 11—interdomain troughs, 12—projections of basite–granulite basement, migmatite–charnockite and migmatite–plagiogranite domains; 13—projections of metabasite–granulite basement and migmatite–enderbite (charnockite) domains; 14—deep fault zones: (a) of first order, mantle origin (1) Lyubeshov–Rudensky, (2) Perzhano–Surozsky, (3) Krivorozhsko–Kremenchugsky, (4) Odessa–Gomel, (b) of second order, crust origin: 5—South Pripyat, 6—Teterev, 7—Central, 8—Khmelnik, 9—Podol, 10—Andrushev, 11—Brusilov, 12—Yadlov–Tractemirov; 15—border faults of PDDB. Study area is shown by rectangles (outer rectangle corresponds to the modelled area and the inner rectangle to the area of gravity calculations).

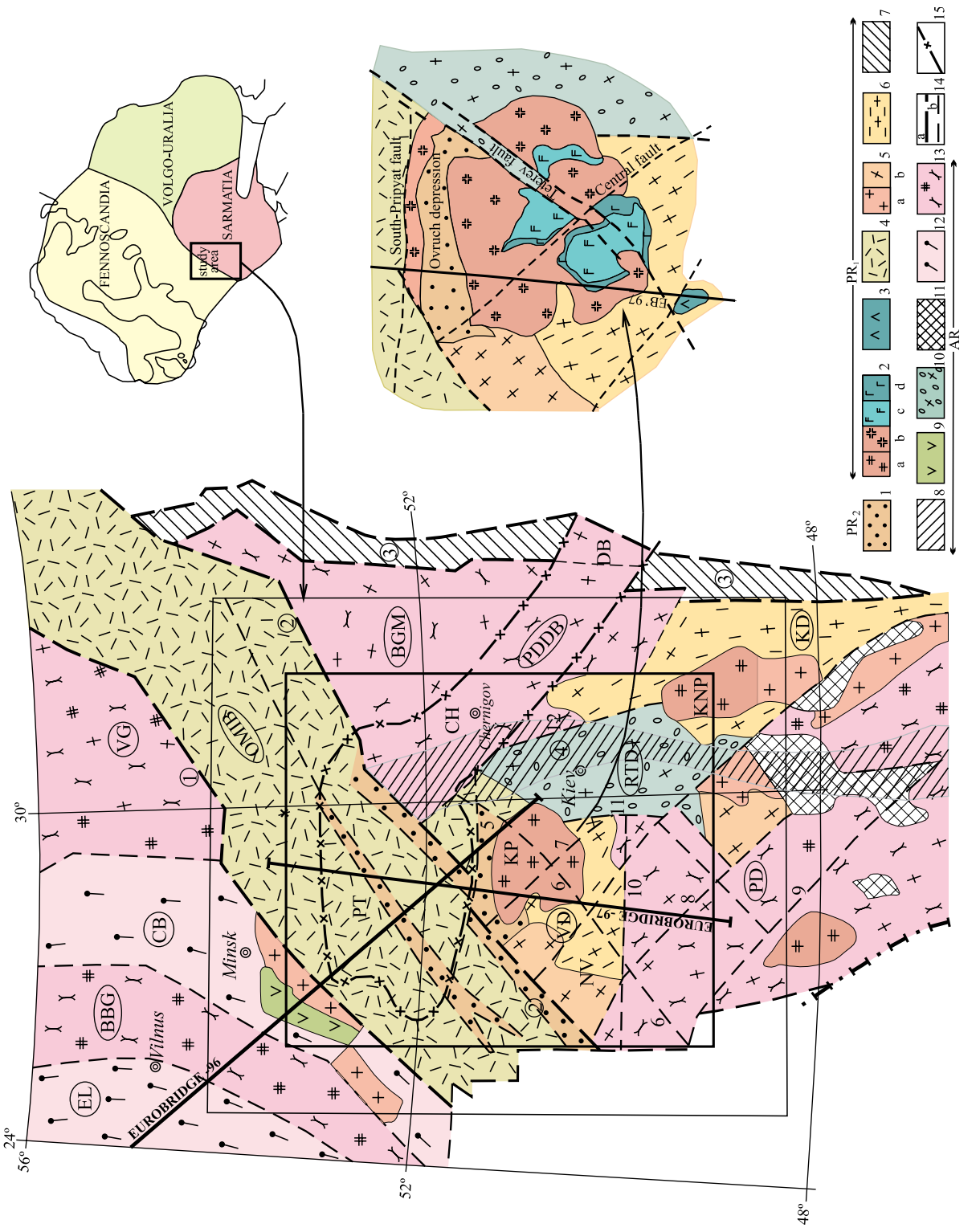
FENNOSCANDIA
VOLGO-URALIA
SARMATIA
study area
South-Pripyat fault
Ovruch depression
Lelchitsy fault
Central fault
EB'97
EUROBRIDGE-96
EUROBRIDGE-97
Minsk
Vilnus
Chernigov
Kiev
EL
BBG
CB
VG
OMIBB
PT
CH
BGM
PDDB
DB
KP
RTDB
KNP
KD
PD
PR1
PR2
AR

2. Geological and geophysical data

2.1. Geological studies

The EB'97 profile crosses the Palaeoproterozoic suture zone between the Fennoscandian and Sarmatian domains (Fig. 1) according to Gorbatschev and Bogdanova (1993). These two domains together with a third one—Volgo–Uralia—comprise the East European Craton (EEC). Gorbatschev and Bogdanova (1993) consider the Fennoscandia–Sarmatia suture zone as the most fundamental large-scale lithospheric boundary in the western part of the EEC. Across this suture, Palaeoproterozoic juvenile crust in Fennoscandia meets the mostly Archean crust of Sarmatia. This crustal discontinuity is marked by the wide Osnitsa–Mikashevichi Igneous Belt (OMIB) of ca. 2.0–1.95 Ga age. According to seismic reflection data in this area, the complex of stacked Fennoscandian terranes plunges southeastwards beneath the edge of Sarmatia (cf. Juhlin et al., 1996).

In the study region, the EB'97 profile crosses three domains, separated by deep fault zones (Fig. 1). The northeastern orientated OMIB is located in the northern part of the region, where metamorphosed sedimentary and volcanic Palaeoproterozoic rocks were intruded by many bodies of granodiorites–diorites in the period 2.0–1.95 Ga. Much of the OMIB in the study region is superimposed by the Palaeozoic Pripyat Trough (PT). The other two domains—Volhyn and Podolian—are related to the Ukrainian Shield. The 3-D density model incorporates additionally the Ros–Tikich Domain of the Ukrainian Shield.

The Podolian Domain (PD) is the oldest block in the region where rocks of granulitic metamorphic grade—mafic granulites and pyroxene-bearing gneisses of Archean age (3.4–2.6 Ga)—are exposed among Palaeoproterozoic granitoids of different composition. This domain represents the oldest stage of evolution of the continental crust with the formation of Archean granulitic cores (Chekunov, 1989).

The Volhyn Domain (VD), located between the PD and the OMIB, is the most controversial one in regard to its crustal history. Most of the available data here indicate the absence or negligible presence of Archean crust. The VD includes mostly gneiss formations of the Teterev complex of amphibolitic metamorphic grade with granitic intrusions of the Zhitomir complex with an age of 2.06 Ga (Shcherbak et al., 1998). Subsequent fault activation, accompanied by anorogenic magmatic activity, represented by intrusions of various composition, from peridotites to granodiorites, is caused by tectonic events occurring within the limits of the OMIB. As a result of a successive stage of tectonic stabilisation of the craton (subplatform stage), terminated by a second episode of anorogenic magmatism (1.8–1.73 Ga), the large, complex Korosten Pluton (KP), composed of rapakivi granites and anorthosites, was formed. At the platform stage, the domain was covered by sedimentary and volcanic rocks. According to Chekunov (1989), the VD represents a stage of mature continental crust.

The Ros–Tikich Domain (RTD), located in the southeastern part of the region, is made up of sedimentary and volcanic rocks subjected to amphibolite-grade metamorphism (amphibole-bearing and biotite gneisses, plagiogneisses and amphibolites). New age determination data of rocks of the RTD (Stepanyuk et al., 1998) point to different times of origin: Archean for the southern part of the domain (synchronous to the gneisses and mafic granulites of the PD), whereas gneisses of the northern part of the domain are similar to Palaeoproterozoic rocks of the VD. Granitoids of the RTD are represented by two groups: plagioclase granites–granodiorites of the Zvenigorod complex and normal granites of the 2.1 Ga Uman complex. The characteristics of the mentioned complexes are presented in Table 1 and Fig. 1.

2.2. Physical properties

Physical properties of rock samples of the study region—density and elastic, magnetic and electric parameters—were systematically studied during the last decades by measurements in the laboratories of the Geological Survey and Academic Institutes of Ukraine. The results have been published in many Russian-language papers and monographs. Physical parameters at high-pressure and high-temperature conditions are reported by Lebedev et al. (1986, 1988).

For the purposes of the gravity modelling, we made a generalisation of P-wave velocity and rock density data in the study region; the results are shown in Table 1 and in Fig. 2. These data are accompanied

Table 1
Physical properties of main rock types for the EUROBRIDGE-97 area

Crustal layer	Age		Complex, series	SiO_2 (%)	Rock types	Physical properties laboratory measured			V_p, (km s^{-1}) according to seismic data on EB'97 pr.	ρ (km m^{-1}) adopted in gravity models	Occurrence (domains)
		Ga				Density ρ, (kg m^{-3})	V_p velocity, (km s^{-1})				
							At $P=1$ GPa	At $P=5$ GPa			
Upper crust ("granite–gneiss" layer)	Proterozoic	1.8–1.75	Korosten complex	68	granite	2610	6.15	6.29		2620	VD
					rapakivi granites	2650	6.37	6.52	6.2–6.4	2620–2650	VD
					anorthosites and gabbro–anorthosites	2720–2790	6.85	6.95			VD
					gabbro–norites	2960	6.95	7.04			VD
					gabbro–peridotites and peridotites	3470–3700					VD
		2.0–1.95	Osnitsa complex	64	granites	2710	6.14	6.33			OMIB, VD
					granodiorites	2720–2740	6.19	6.36	6.1–6.3	2740	OMIB, VD
					diorites	2850	6.30	6.53		2780–2800	OMIB, VD
		2.06–2.08	Zhitomir complex	68	biotite granites, plagiogranites and migmatites	2630–2650	6.0–6.2	6.2–6.4	6.1–6.2	2650	VD
		2.02–2.08	Berdichev complex	67	garnet–biotite granites	2740	6.25	6.45	6.1–6.2	2740	PD
					charnockites, enderbites	2740–2780	6.34	6.48	6.2–6.4	2760–2780	PD
		2.4	Teterev series	67	biotite gneisses, biotite–plagioclase gneisses	2650–2770	6.18	6.34	6.2	2670	VD, RTD
Lower crust ("granulite–basitic" layer)	Archean	2.4–2.7	Ros–Tikich series (of amphibolitic metamorphism)	58	biotite gneisses, biotite–plagioclase gneisses	2730	6.17	6.33			RTD
					biotite–amphibole gneisses, amphibole–plagioclase gneisses, amphibolites	2790–2950	6.25–6.3	6.4–6.5			RTD
		3.1	Gaivoron complex		enderbites	2740–2760	6.24	6.48	6.2–6.4	2760–2780	PD
		3.4	Dnestr–Bug series (of granulitic metamorphism)	58	mafic granulites (two–pyroxene gneisses, amphibole–pyroxene gneisses, pyroxene–plagioclase gneisses)	2950–3100	6.8–7.0	6.9–7.2	6.8–7.1	3000–3100	PD, RTD
			Complex of mafic and ultramafic rocks	42	gabbro–norites, pyroxenites	310–3200	6.9	7.4	7.4–7.6	3.15–3.20	PD, RTD

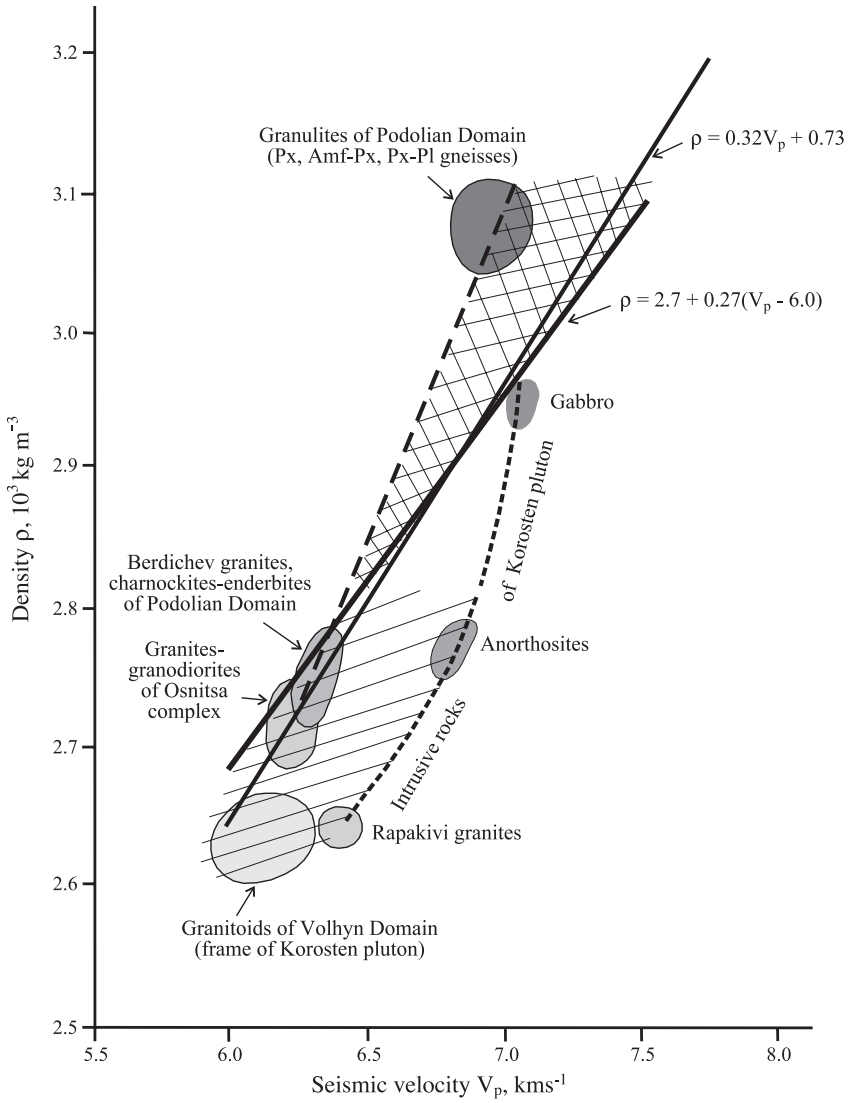

Fig. 2. Diagram of the density/velocity relation of major rock types for the EUROBRIDGE-97 area. Intrusive rocks of Korosten Pluton (rapakivi granites and anorthosites) and granitoids of the Volhyn Domain have reduced densities (thin lines area) in comparison with standard functions (thick lines), whereas the granulites of the Podolian Domain have increased densities (crossed lines area).

by values of the average silica content (SiO_2) of the main lithological complexes (Kulish and Gorlitsky, 1989), which is the most important characteristic of the rock composition.

Granitoids are the most widespread rock type in the region. They represent the upper ("granite-gneiss") layer of the crust with V_p=6.0–6.4 km s^{-1}, ρ=2600–2750 kg m^{-3} and $SiO_2 \approx 68–64\%$ (Table 1). According to the density values, two groups of rocks can be distinguished: (1) granites of normal and decreased densities of the VD (biotite granites of Zhitomir complex and rapakivi granites of KP) with $\rho \leq 2650$ kg m^{-3}; and (2) anatectic granitoids of the PD (Berdichev granites, charnockites–enderbites) and granites–granodiorites of the OMIB with $\rho = 2700–2750$ kg m^{-3}. Rocks, which according to their parameters (V_p=6.4–6.8 km s^{-1}, ρ=2780–2900 kg m^{-3}, $SiO_2 \approx 62\%$) may characterise the middle crust ("di-

oritic" layer), are poorly investigated and, for this reason, they are not presented in Table 1. In the study region, they are represented by charnockites, biotite–plagioclase gneisses, diorites, and enderbites. These rock types are similar to those observed in parts of the Voronezh Massif (located to the northeast of the Ukrainian Shield) and the Baltic Shield (Krasovsky, 1981) for which data relating to physical properties are available.

Lower crust ("granulite–basite" layer) in the study region may be represented by Archean mafic granulites (two-pyroxene, amphibole–pyroxene, pyroxene–plagioclase gneisses and crystalline schists) with $V_p = 6.9–7.2$ km s^{-1}, $\rho = 2950–3100$ m^{-3}, $SiO_2 \approx 56–57\%$, exposed at the surface in the PD, and Archean complex of mafic and ultramafic rocks (gabbro–norites, dunites, peridotites, and pyroxenites with $V_p = 7.8–8.0$ km s^{-1}, $\rho = 3200–3300$ kg m^{-3}, $SiO_2 \approx 42\%$) exposed in the RTD as remnants and xenoliths within Palaeoproterozoic granitoids. Naturally, to predict the composition in the middle and lower crust, we have to use physical parameters (first of all velocity) measured or corrected with regard to temperature–pressure conditions at corresponding depths.

An important aspect of the gravity modelling is to take into account the physical properties of specific rock types comprising the geological units of the domains. Fig. 2 illustrates the distribution of velocity and density of the main rocks in the study region relative to the functions $\rho = 320$ (V_p)+730 kg m^{-3} (Krasovsky, 1981) and $\rho = 2700+270$ ($V_p-6.0$) kg m^{-3} (Gordienko, 1999; Yegorova et al., 1997), which are adopted as standard relations. Only the rocks of the OMIB, Berdichev granites, and charnockites–enderbites of the PD have velocity/density relationships distributed very close to these regression lines. Granitoids of the VD, and, especially, rapakivi granites and anorthosites of the KP are characterised (Yegorova, 1993) by decreased densities (in Fig. 2, they are shifted towards the increased P-wave velocity), whereas mafic granulites of the PD, in contrast, have increased density values in comparison with that predicted by standard functions. This suggests that the ρ/V_p relation in separate blocks strongly differs from standard functions used in initial gravity models, but the determination of this relation can only be realised in the course of fitting the density models.

2.3. Characteristics of gravity and magnetic fields

As initial gravity data we used Bouguer gravity maps (with reduction density 2670 kg m^{-3}) at 1:1,000,000 scale with contour interval 2 mGal (rms ≈ 0.7 mGal). For the purposes of gravity modelling, these data were averaged on a 20×20 km grid. The accuracy of this averaged field allows constructing maps with a contour interval of approximately 5 mGal (Fig. 3). By such a procedure, we have filtered out local anomalies and highlighted anomalies caused by deeper (lithospheric) structures. Fig. 3 shows the boundaries of domains in the study region, outlined with regard to gravity and magnetic field patterns, thus reflecting deep constraints on the domains. That is why the configurations of the domains in Fig. 3 look somewhat different from those in Fig. 1, which were distinguished according to subsurface geological data.

The most expressive feature of the observed gravity field (Bouguer anomalies) g_{obs} of the study region is the Chernigov high of over 80 mGal in amplitude, which is the strongest gravity anomaly over the East European Platform. Since its origin is well-studied (Chirvinskaya and Sollogub, 1980), this anomaly will be considered in connection with the interpretation of other anomalies of the region. To the west of the Chernigov high, a gravity low over the PT with two separate minima—the northern (−65 mGal) and the southern (−55 mGal)—can be seen in Fig. 3. The latter adjoins a gravity low, defined by the zero contour, over the KP, whose amplitude increases northward reaching −20 mGal. To the west of the KP, one can distinguish the strong Osnitsa high (50 mGal) of somewhat triangular configuration and a predominance of northeastern orientations corresponding to the general trend of the OMIB. The same direction is typical for the intermediate zone of the Novograd–Volhyn block (being a segment of the VD) with average g_{obs} of about 10 mGal. Over the PD, there are two areas of high g_{obs} each attaining 30 mGal. The first of these encompasses the province of Berdichev granites in the southwest and the second, corresponding with the regional Vinnitsa magnetic anomaly, relates to the exposure of charnockites–enderbites.

Over the RTD, the main gravity anomaly trend changes to north–south and corresponds well with the

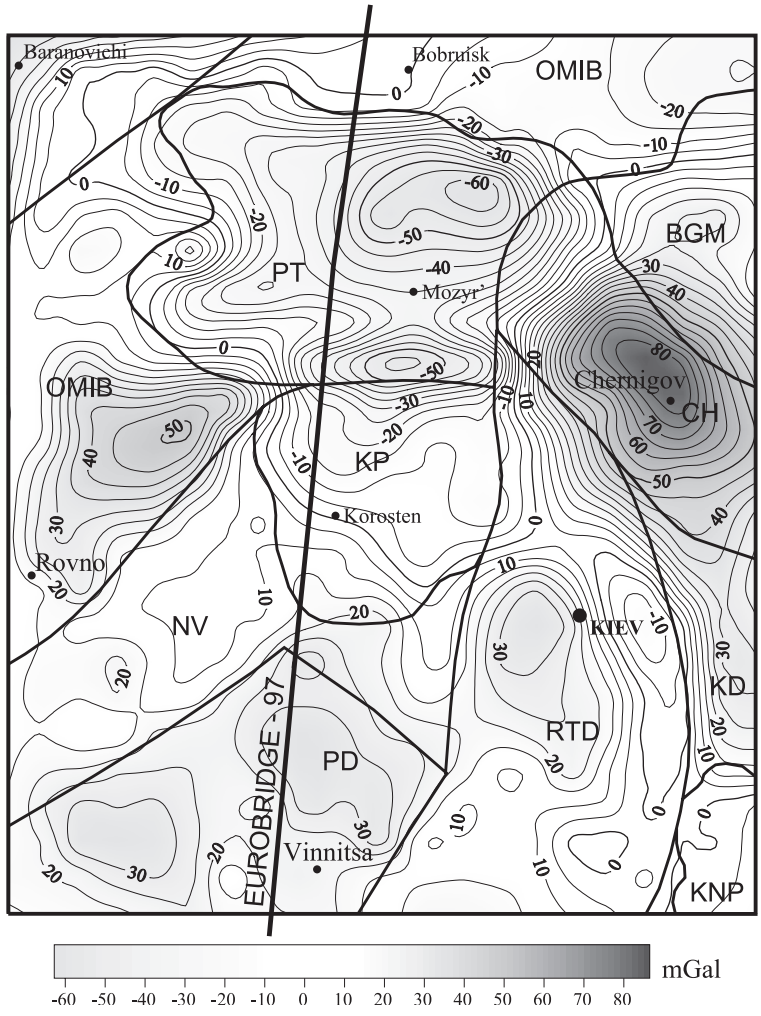

Fig. 3. Observed gravity field (Bouguer anomalies averaged on 20×20 km grid), mGal, used in 3-D gravity modelling for the EB'97 region (inner rectangle in Fig. 1). Contours of main domains are outlined by solid lines. BGM—Bragin Granulite Massif, CH—Chernigov block of the Dnieper–Donets Basin, KD—Kirovograd Domain, KNP—Korsun–Novomirgorod pluton of the KD, KP—Korosten Pluton of the Volhyn Domain (VD), NV—Novograd–Volhyn Domain of the VD, OMIB—Osnitsa–Mikashevichi Igneous Belt; PD—Podolian Domain, PT—Pripyat Trough, RTD—Ros–Tikich Domain.

pattern of the magnetic field. There are two principal anomalies here: one, covering the area of positive g_{obs} values (30 mGal), adjoins the PD, whereas a second, narrow gravity low of −10 mGal in the eastern part of the domain relates to the boundary zone between the RTD and Kirovograd domains (KD).

Magnetic anomalies in the northwestern part of the region have a general northeastern orientation corresponding with the overall trend of the OMIB. According to the character of magnetisation, two different regions, separated by the Perzansky fault (incorporated as part of fault zone 2 of northeast orientation in Fig. 1), are distinguished (Orlyuk and Pashkevich, 1996, 1998). The mosaic pattern of the OMIB magnetic field is caused by diorite bodies and gabbro intrusions extended along the general orientation of the belt. Magnetisation intensity of the lower crust is estimated to be 1–2 A/m (Orlyuk and Pashkevich, 1996). The mosaic magnetic field of the VD can be seen against the background of the regional Novo-

grad–Volhyn magnetic anomaly (in the southwestern part of the domain) and the negative magnetic field over the non-magnetic rocks of the KP (in the northeastern part). The sources of local magnetic anomalies are mostly mafic intrusions during the unstable platform stage of evolution. The lower crust of the Novograd–Volhyn block is highly magnetised (up to 3 A/m), whereas within the KP the magnetisation of the lower crust changes from practically non-magnetic to the northeast to 2 A/m to the southwest.

The crust in the area of the Berdichev granites, which is non-magnetic over its whole thickness, meets the Vinnitsa block, marked by a regional magnetic anomaly, where Archean mafic granulites are exposed at the surface; magnetisation of the lower crust reaches 3 A/m. The magnetic field of the RTD is heterogeneous. In its southern part, strong local anomalies, caused by granulitic rocks, complicate the regional Gaysin magnetic high. Local magnetic anomalies in the northern part of the domain are mainly caused by metavolcanic rocks.

2.4. Seismic data

The study region is crossed by DSS profiles II, IV and VI (Fig. 4) that were acquired in the 1980s. These

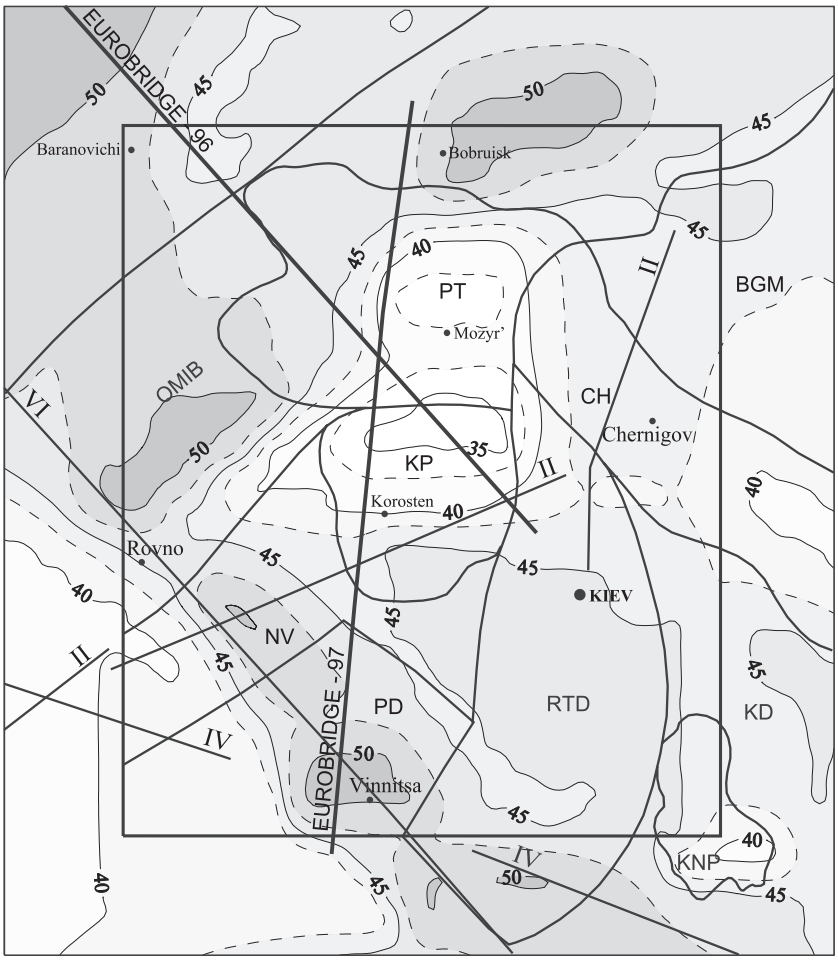

Fig. 4. Moho map used in 3-D density modelling the crust of EB'97 region, contour values in km (Chekunov, 1992). Domains are abbreviated as in Fig. 3. The location of the DSS profiles II, IV and VI are shown by solid lines; thick lines indicate the EB'97 profile. Inner rectangle is the area of gravity effect calculation and the outer one indicates the limits of the density model.

profiles were interpreted by different authors using various methodologies, leading to variable results. Seismic boundaries within the crust were identified, mainly from reflected waves, with recent crystalline basement, ancient crystalline crust (protobasement), and with the top of the basaltic layer (Chekunov, 1987, 1988).

The Moho surface shown in Fig. 4 was constructed mainly from reflected waves (Chekunov, 1987, 1988, 1992) since the acquisition style did not allow recording refracted phases from the Moho boundary over sufficiently long distances. Other geophysical data were also used (Chekunov, 1992). It can be seen in Fig. 4 that Moho depths below the OMIB increase to 50 km and more, whereas average depths beneath the PD and RTD are about 45 km. Against this background, the PT and KP are outlined by a Moho uplift to a depth of 35–37 km.

2-D gravity modelling, carried out along the DSS profiles II, IV and VI (Chekunov, 1987, 1988; Krasovsky, 1981), revealed a complex density distribution in the crust both throughout its entire thickness as well as in separate crustal blocks; especially large density variations are typical for the upper crust. The KP is an exception from this regularity; it corresponds to lighter crystalline crust. A clear correlation between the subsurface geological structure and densities to depths of 10–15 km was noted by Krasovsky et al. (1998).

3. Three-dimensional gravity modelling of the Earth's crust of study region

3.1. Modelling methodology

3-D gravity modelling of the study region was approached by setting up a regional structural background to the EB'97 profile. The target of the modelling was to find a density distribution for the whole crust consistent with the gravity observed field (within permissible error limits) and with available geological constraints. To fulfil this work we used gravity a backstripping analysis—i.e. a priori removal of the effects of the main crustal layers, whose structure and parameters are geophysically and geologically constrained followed by the analysis of the obtained residual anomalies in terms of density heterogeneities in lower crustal layers. The 3-D gravity modelling was carried out using an automated system (Starostenko et al., 1997), the core of which contains programs for solving the direct gravity problem for a prism of variable density distribution with depth (Starostenko and Legostaeva, 1998a), including exponentially (Starostenko and Legostaeva, 1998b). See also Starostenko et al. (2004).

The 3-D modelling was carried out at the scale of 1:1,000,000 (20×20 km data averaging). The initial model comprised three layers: (1) sediments, where thickness varies from 100 m on the Ukrainian Shield to 5–6 km in the PT; (2) an upper layer of crystalline crust, whose heterogeneities are the sources of the main gravity and magnetic anomalies, with a base adopted at a depth H of 15 km; and (3) a lower crustal layer bounded by the Moho.

The gravity effects of these layers were calculated according to anomalous densities $\Delta\rho$, obtained by normalising absolute density values to a standard based on average Precambrian craton crustal structure (Kozlenko, 1986)—given by $\rho(H)$ where density gradually increases from top to bottom (40 km) in the range 2700–2940 kg m^{-3}. Upper mantle density was adopted as 3350 kg m^{-3}. The use of this relationship, which is the upper part of the PEM-C model of Dziewonski et al. (1975), gives the calculated gravity effect at an absolute level, one that is directly comparable with the observed Bouguer anomaly field. Note that this is just a purely "technical" procedure to simplify the calculations. The particular approach used to normalise absolute density values depends on the preferences of the interpreters, some of whom, for example, use a $\Delta\rho$ related to upper mantle density. In any case, at the end of the calculations the $\Delta\rho$ values were converted back into absolute values, which are shown in the figures demonstrating the density distribution of crustal layers.

The model is defined inside the outer rectangle, while the gravity effect was calculated within the limits of the inner one (cf. Figs. 1 and 4, and others) meaning that the model is framed on all sides by a "fringe" of 80 km width.

3.2. Removing the effect of the sedimentary cover (gravity "backstripping")

The two main gravity anomalies of the study region—the low over the PT and the Chernigov high—

correspond, respectively, to the location of greatest thickness of the sedimentary cover (5–6 km) in the PT and in the northwestern segment of the Dnieper Basin (DB; Fig. 5). Although these elements are compound segments of the single Pripyat–Dnieper–Donets Basin (PDDB), their structure and evolution are considered to be different (Chekunov, 1994; Stephenson et al., 1993). In particular, this is indicated by the change in trend of the PDDB at the Chernigov–Bragin swell from E–W in the PT to NW–SE in the DB. The thickness of sediments reaches 6 km in the axial part of the northwestern DB, whereas in the PT the maximum thickness (up to 6 km) occurs near the flanks of the basin in two local depressions, separated by a basement uplift (up to 3 km) along the axis of the basin.

Two versions of a sedimentary cover model were considered, adopting different density distributions: in one an average layer density was used and in the other

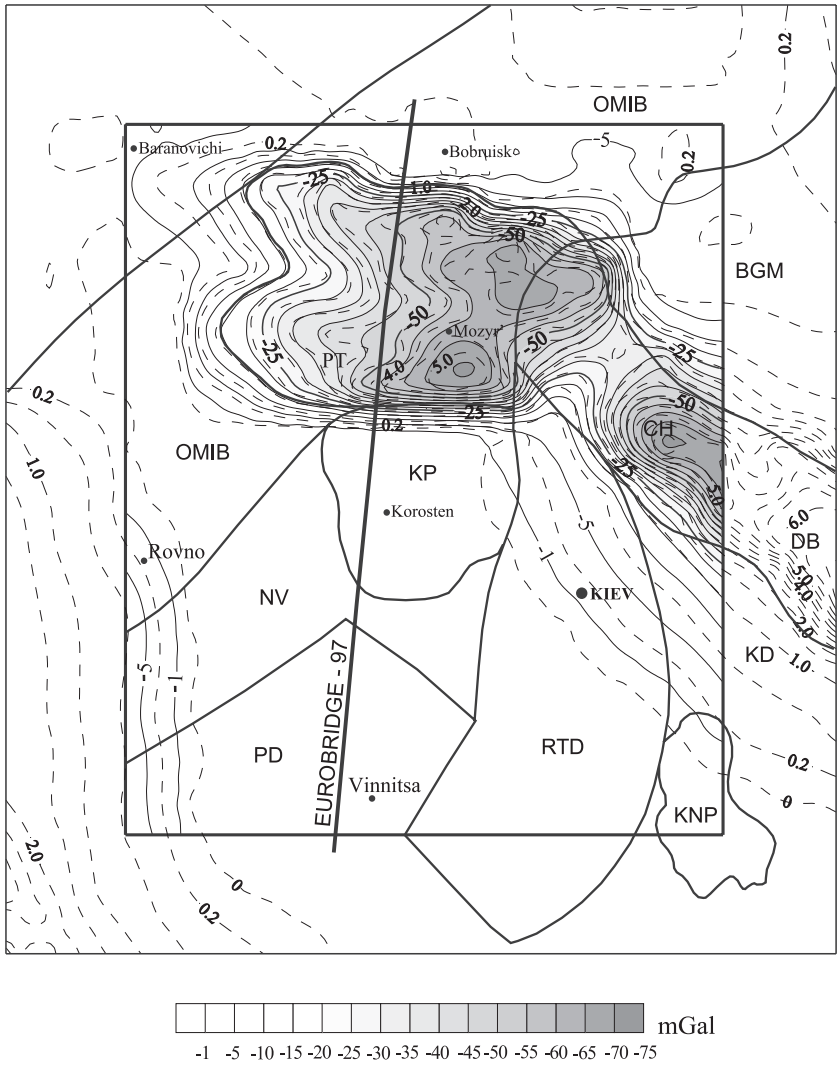

Fig. 5. Gravity effect of the sedimentary cover (solid lines, main contour interval 5 mGal) and thickness of the sedimentary cover (depth to crystalline basement in km; dashed lines).

density was assumed to increase with depth according to an exponential function. Fig. 5 shows the thickness of sediments and corresponding gravity effect using an average density of 2350 kg m^{-3}. The PT is clearly distinguished by Δg_{sed} low of −55 mGal, conforming to the pattern of both basement depth and observed gravity field. It is evident that the PT gravity low is mainly caused by the influence of the interface between sediments and crystalline basement.

An anomaly Δg_{sed} of the same magnitude (≈ -60 mGal) is revealed over the Chernigov high. In the residual field Δg_{res} (Fig. 6a), obtained by subtracting the effect of sediments Δg_{sed} (Fig. 5) from the observed field g_{obs} (i.e. $\Delta g_{res}=g_{obs}-\Delta g_{sed}$), the Chernigov high manifests itself by increasing its amplitude up to 140 mGal, whereas the gravity low over the PT practically disappears. In the southern part of the PT, a narrow strip of positive Δg_{res} anomalies of 30–35 mGal amplitude joins the Osnitsa and Chernigov highs (Fig. 6a). The latter anomaly is known to be the extreme northwestern segment of a chain of axial gravity highs over the DB caused by mafic and ultramafic rocks intruded into the crystalline crust during Palaeozoic rifting (Starostenko et al., 1986; cf. Yegorova et al., 1999). Thus, removal of the sediment layer effect indicates an absence below the PT of an axial high-density body of similar origin to that below the DB. The DB axial body terminates in the vicinity of the Chernigov gravity high and is probably constrained by the deep N–S-orientated Odessa–Gomel tectonic zone. According to Bogdanova (1984), this zone separates granulitic–mafic (to the west) and greenstone (to the east) crustal domains. Clearly, rift-related mafic intrusion of the crust be-

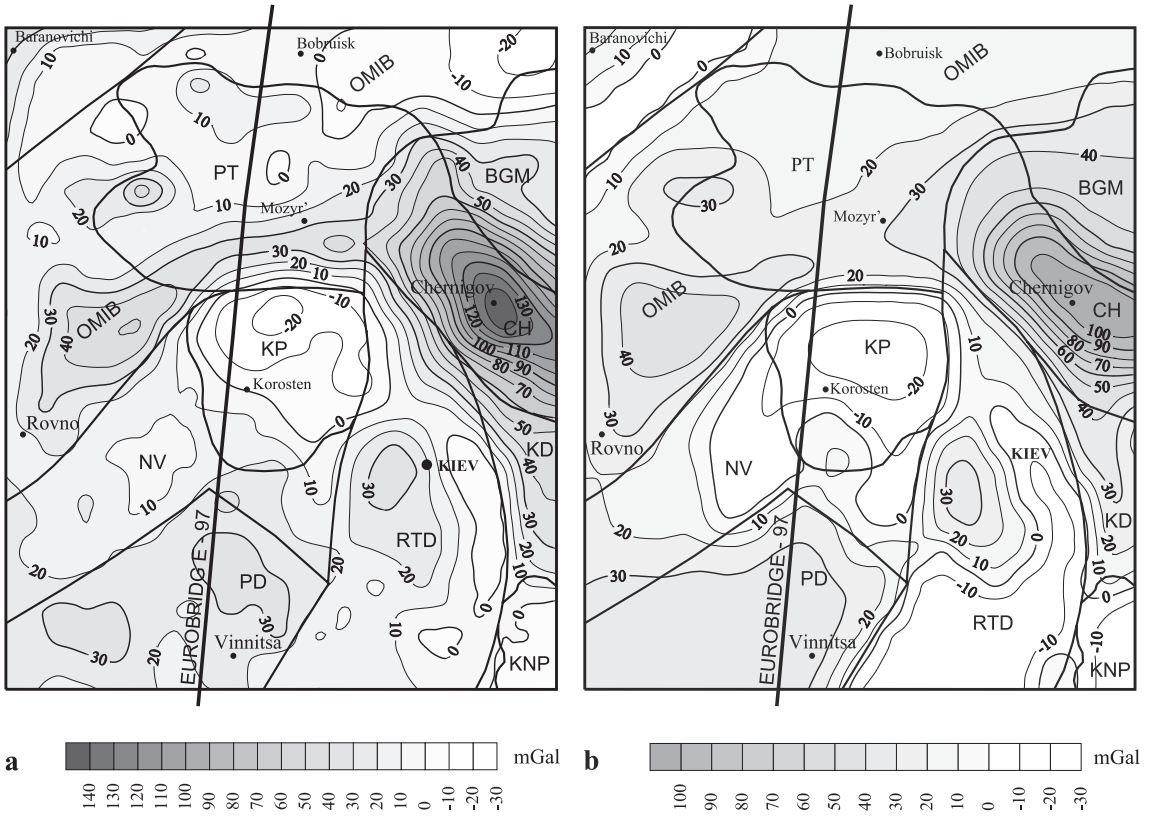

Fig. 6. (a) Residual gravity field in mGal, obtained by removing the gravity effect of sediments (Fig. 5) from the observed field (Fig. 3), and (b) gravity effect of the upper crystalline crust, with its base at 15 km, in mGal, from the heterogeneous density distribution shown in Fig. 7.

neath the PT is less profound, if it occurred at all, than beneath the DB. We assume that local magmatic bodies were intruded not under the central part of the PT (as in the DB), but mainly in a zone parallel to the South Pripyat Fault (SPF).

Removal of the effect of the sediments of the PT has led to a reorganisation of the gravity pattern over the KP with the formation of an isometric low with extreme values of −25 mGal located over the northern part of the pluton adjacent to the PT (Fig. 6a). This may be indicative of the maximum thickness of rapakivi granites (of 1.75 Ga age) in this area and, probably, that the emplacement of acid magmas may have been controlled in part by the E–W SPF.

In general, the division of the crust in the study region into its main crustal domains is seen more clearly in the residual gravity field (Fig. 6a) than in the observed field (Fig. 3). Subsequent gravity modelling, in which the density distribution within the crust was inferred, was carried out in respect of the residual field Δg_{res}.

3.3. Modelling of the upper crust

Interpretation of the residual gravity field Δg_{res} (Fig. 6a) was made assuming that the main local anomalous masses are distributed in the upper crustal layer (Krasovsky, 1981; Krutikhovskaya et al., 1982), which extends to a depth of about 15 km. The choice of this depth as a lower boundary was based in part on a seismic horizon observed in the Ukrainian Shield at a depth of 12–15 km (Chekunov, 1988). According to Pavlenkova (1988), this interface (called K_1) divides an upper crust of blocky structure from a middle and lower crust of mainly layered structure. Block structures are characterised by steep boundaries, whereas the layered structures of the middle and lower crust are characterised by boundaries having horizontal to subhorizontal attitudes.

Model densities for the upper crust are based on laboratory measurements for the main rock types of the study region (see Table 1), generalised in a rock-density map of the Ukrainian Shield (A.O. Shmidt, personal communication). This scheme was adopted as an initial density distribution at the top of the upper crystalline crustal layer. In the course of modelling, this was modified with regard to geological setting and gravity field character. The initial version of the model incorporates a heterogeneous density distribution at the top of the crystalline basement (Fig. 7a), which increases with depth to a uniform value of 2790 kg m^{-3} at a depth of 15 km (according to the corresponding reference density, see Section 3.1). This means that the tops of geological units have been assigned densities based on measurements from surface samples and that these densities increased with depth within each geological unit. An exception is in the area of the Chernigov high where densities at the top of the crystalline basement ($\rho = 2900$ kg m^{-3}) are decreased slightly, in keeping with the assumption of a rather shallow occurrence of granulitic rocks here. The calculated gravity effect of the initial density model compares quite well in terms of pattern with the residual field Δg_{res} in Fig. 6a, but amplitudes of the calculated highs are only half of the Δg_{res} values (the modelled Chernigov high attained only 45 mGal).

A second approach adopted the same densities at the top of basement as in the initial version (i.e. laterally varying, according to the geology) but did not constrain them to be equal at the base of the model layer (at 15 km depth). Rather, the surface density contrast was maintained throughout. The density distribution at the base of the layer (H=15 km) is shown in the lower panel of the block-diagram (Fig. 7b). The gravity effect of this model Δg_{upcr}, seen in Fig. 6b, corresponds well with the Δg_{res} field (Fig. 6a), in terms of both configuration and amplitude. The mean difference of these two fields is ±10 mGal. The distribution of deviations has a mosaic pattern. There is no correlation between deviations and geological units, with the exception of the residual anomaly of 40 mGal in the region of the Chernigov high, which may point to the presence of dense rocks in the lower crust there.

The main result of the upper crustal modelling is that the general features of the residual field can be explained by density heterogeneities at this depth. The main features of the inferred density distribution are as described below.

The highest densities (up to 3000 kg m^{-3}) are found in the upper crust of Chernigov segment of the PDDB (Fig. 7). The Chernigov segment occurs in an area with granulitic basement (ρ=2780 kg m^{-3})—the Bragin Granulitic Massif (BGM). The extremely high density of the rocks of Chernigov segment is inter-

preted to be the result of the reworking the granulitic basement due to intrusions of mafic and ultramafic rocks during Late Palaeozoic rifting. The Chernigov–Bragin Swell is perhaps comparable with the Rhine Massif. Consolidated basement in both blocks is uplifted, they both separate rift basins of different orientation—the Dnieper and Pripyat basins and the Upper and Lower Rhine Grabens, respectively. Widespread development of volcanic rocks in the latter has formed the Vogelsberg volcanic shield and Westerwald volcanic province. Similar features—Chernigov–Gribova Rudnya and Vediltsy–Ladinka—are also observed in the Chernigov–Bragin Swell (Kozlenko, 1989).

To the south, approximately from the Chernigov segment to the Korsun–Novomirgorod pluton, a N–S elongate zone of dense rocks ($\rho \approx 2780$ kg m^{-3}), 30–40 km wide, correlated with a local 30–35 mGal

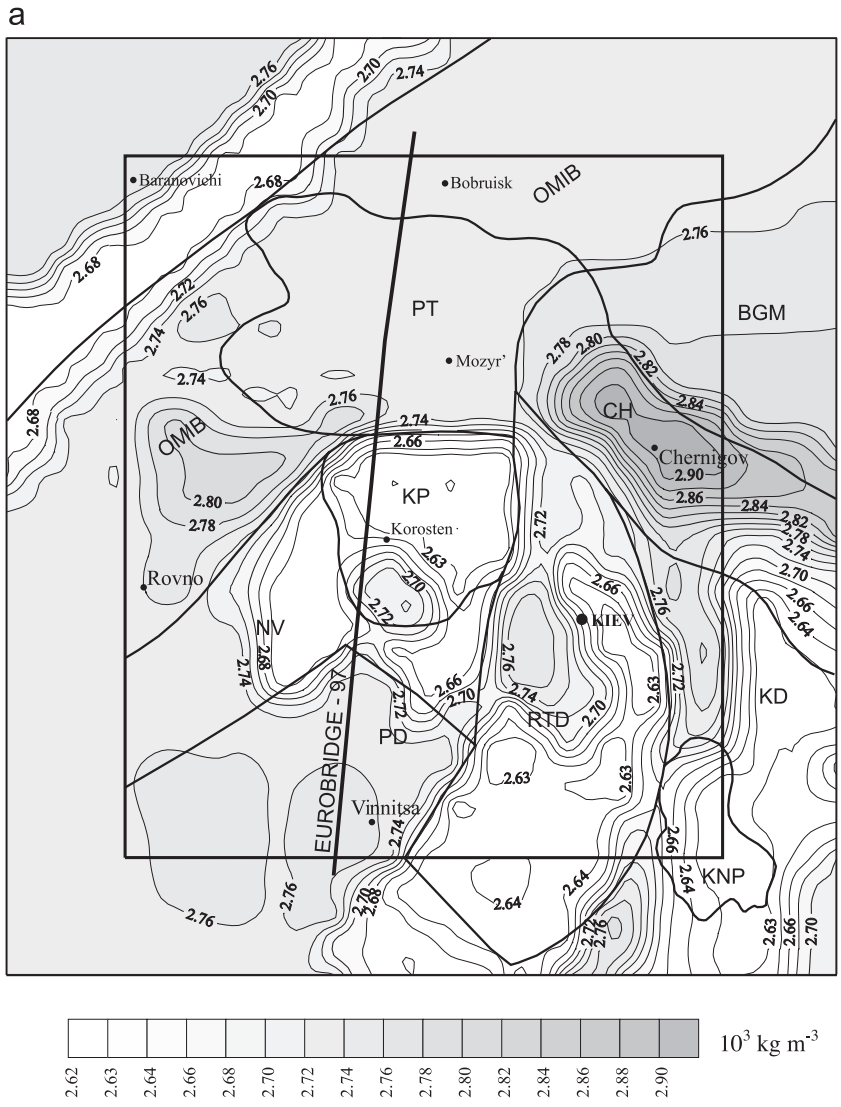

Fig. 7. Distribution of density heterogeneities (10^3 kg m^{-3}) in the upper crystalline crust: (a) and the upper panel of (b) is the density distribution at the top of the upper crystalline crust and the lower panel of (b) is the density distribution at the depth of 15 km.

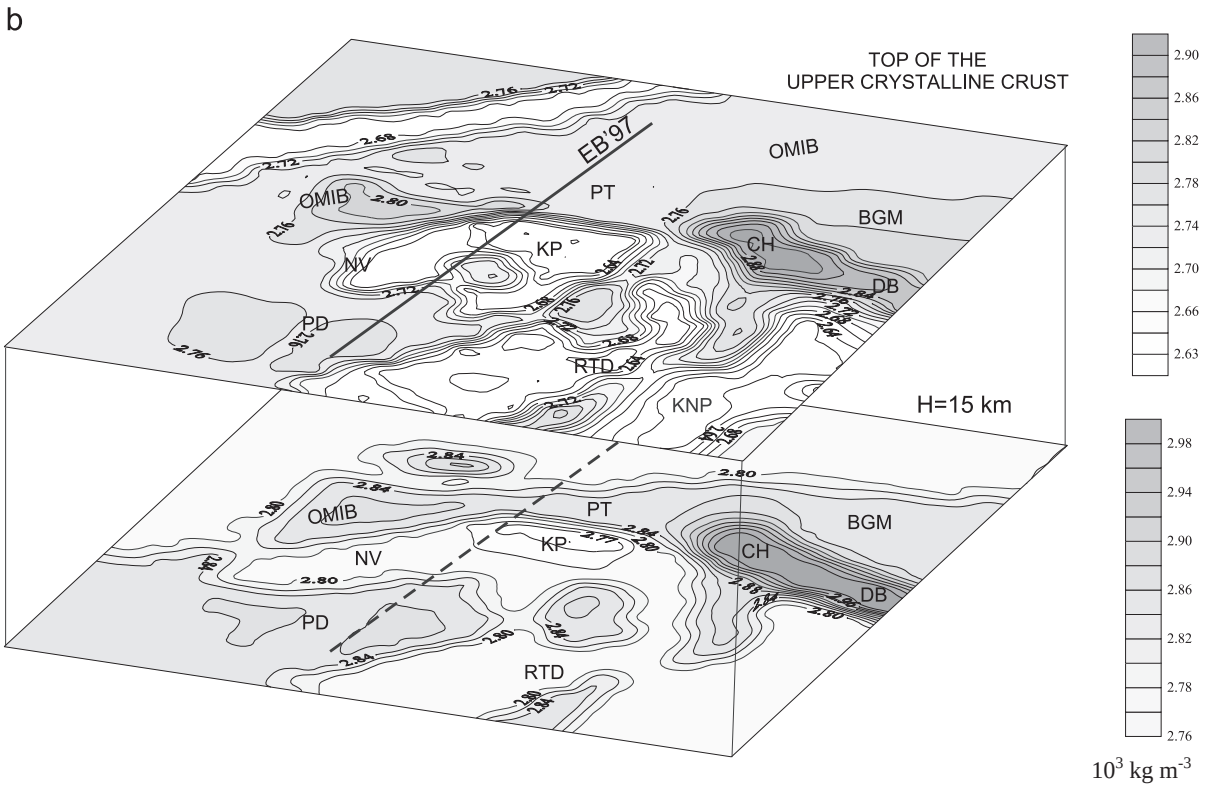

Fig. 7 (*continued*).

gravity anomaly, is inferred. Along the western border of this zone, marked by the Yadlov–Tractemirov fault (fault 12 in Fig. 1), dividing the RTD and the northern part of the Kirovograd Domain (KD), bodies of Archean mafic granulites and ultramafic rocks (dunites, peridotites), being the sources of known magnetic anomalies, are exposed. Compared to the magnetic anomalies, which are of local character, the gravity signature of this zone and, correspondingly, the area of dense rocks, is wider and probably reflects the development of granulites in the upper crust in the limits of the whole zone, superimposed by sedimentary-effusive rocks of the Ingul–Inguletsk series.

High-density upper crust is generally typical for the Archean granulitic basement of the PD (Fig. 7). Above this basement, at the surface, Berdichev granites with $\rho = 2740$ kg m^{-3} and exposures of Archean enderbites (Nemirov complex) of $\rho = 2770$ kg m^{-3} are observed in areas corresponding to increased gravity anomalies (to 30 mGal). The density increase to 2840–2860 kg m^{-3} in the PD at a depth of 15 km may be indicative of a predominance of charnockite–enderbite rocks at the base of the upper crust.

The gravity field of the OMIB is controlled mainly by granodiorites and granites of the Osnitsa complex with $\rho \approx 2740$ kg m^{-3} increasing to 2800 kg m^{-3} at a depth of 15 km. Against this regional background, the Osnitsa gravity high (≈ 60 mGal; see Fig. 3) and another gravity high to the north (up to 20 mGal), are caused by large dioritic batholiths of average density 2800 kg m^{-3} at the top and 2860 kg m^{-3} at the base of the layer.

Low density upper crust (2630–2650 kg m^{-3} at the top to 2800 kg m^{-3} at $H = 15$ km) is typical for the area of Zhitomir complex granitoids in the southern part of the RTD and in the Kirovograd Domain (KD), as well as for the southern frame (biotite gneisses and calciphyres of Teterev series) of the KP.

The least dense upper crust is predicted under much of the northern area of the KP and below the

similar Korsun–Novomirgorod pluton, which is located on the southeastern edge of the study region. They are characterised by density variations from 2630 kg m^{-3} at the surface to 2770 kg m^{-3} at 15 km depth (Fig. 7). Our calculations show that the isometric low seen in Δg_{res} field over the KP, with maximum amplitude −25 mGal in its northern part (Fig. 6a), is explicable by a predominance of rapakivi granites in the northern part of the pluton and by anorthosites in its southwestern part, separated by the Central Fault of northwestern orientation (fault 7 in Fig. 1). The localisation of the Δg_{res} low substantiates the above assumption that the source for acid magmas was located in the northern part of the pluton and was controlled by the E–W orientated SPF. The fault was repeatedly activated, first at the subplatform stage of evolution of the craton (early Proterozoic) in connection with the formation of the OMIB and intrusion of KP, and, later, in Palaeozoic times with the rifting in the PT. Mafic magmas, which have formed the anorthosite massifs in the central and southern parts of the pluton, were intruded along the intersecting

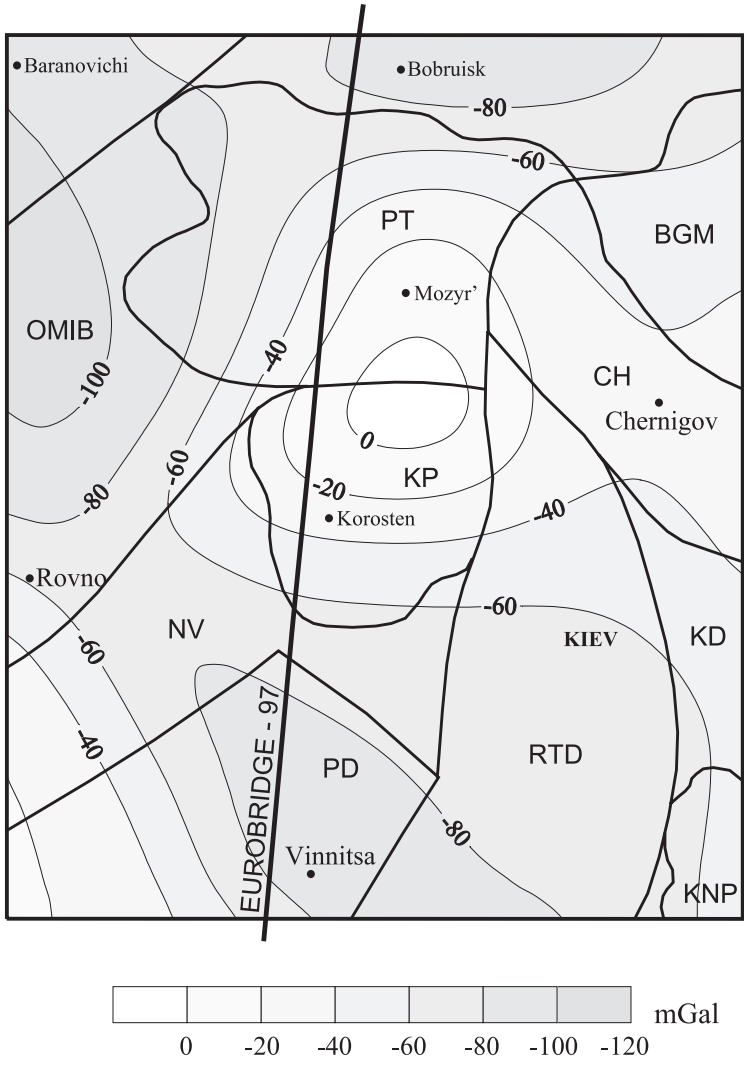

Fig. 8. Calculated gravity effect of Moho topography as given in Fig. 4 (mGal); calculation area corresponds to the inner rectangle in Fig. 4.

diagonal formed by the Teterev and Central faults (Gintov et al., 1974; cf. Bogdanova et al., 2004). Thus, it is evident that intrusion of mafic and acid magmas were controlled by faults of different orientation.

3.4. Estimation of density heterogeneities in the lower crust

As shown above, the residual field anomalies ($\Delta g_{res}=g_{obs}-\Delta g_{sed}$) can be explained by density heterogeneities in the upper crustal layer H=0–15 km. It follows that, if the middle and lower crust includes density heterogeneities, the gravity effects of these have to be mutually compensated. It is assumed that mass balance in the crust is reached at the Moho boundary. Given constraints on Moho structure, the allocation of mass within the layer bounded by H=15 km and the Moho, are now estimated using our 3-D modelling methodology. However, the Moho boundary of Chekunov (1992) shown in Fig. 4, constructed mainly on the basis of reflected waves and not

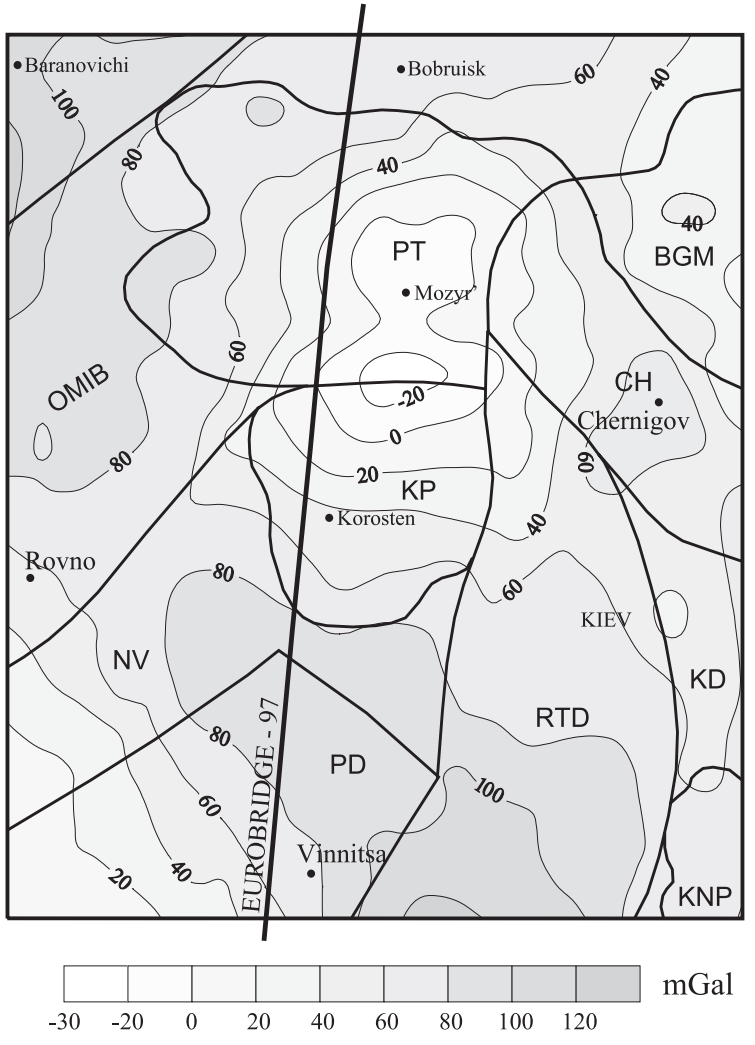

Fig. 9. Effect of lower crustal heterogeneities (mGal) distributed in the layer confined by the depth level H=15 km and the Moho boundary, obtained by subtracting the effect of both sedimentary and upper crystalline crustal layers from the observed field.

controlled by refracted waves, cannot be considered to be very reliable. Changes in this Moho map will lead to changes in crustal density distribution derived by using it.

The gravity effect calculated from the Moho geometry of Fig. 4 is shown in Fig. 8. Zones of increased (to 50 km) crustal thickness correspond to negative anomalies as low as −100 mGal while the mapped Moho uplift produces a gravity high delineated by the −20 mGal contour. To compensate these anomalies, density heterogeneities need to be placed in the lower crust. In order to do this, the gravity effect Δg_{lwcr} caused by lower crustal density heterogeneities is first calculated, as follows. The gravity effect of the mapped Moho Δg_{Moho} (Fig. 8) was removed from the residual field Δg_{res} (Fig. 6a) giving the gravity effect of the whole crystalline crust, $\Delta g_{\mathrm{cr}} = g_{\mathrm{res}} - \Delta g_{\mathrm{Moho}}$, and, in turn, removing the effect of the upper crust Δg_{upcr} (Fig. 6b) from the this gives the anomalous field sourced by lower

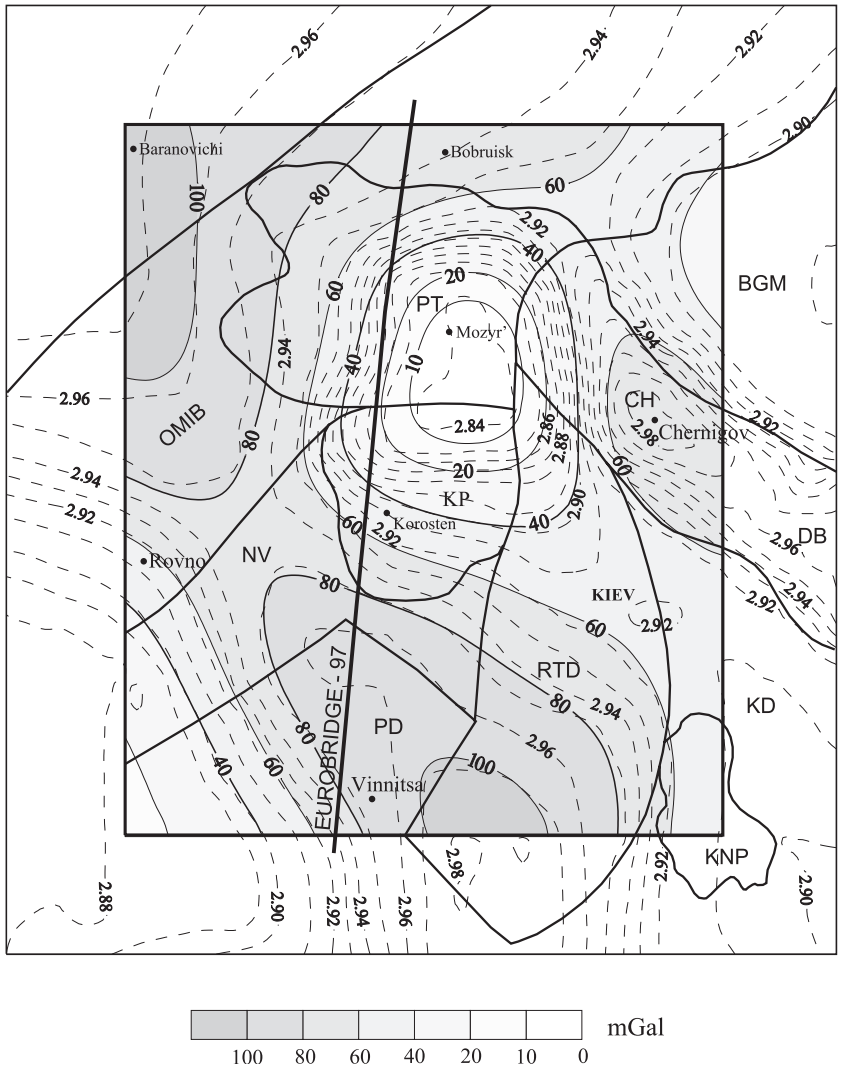

Fig. 10. Calculated residual gravity effect of the lower crust (solid lines within the inner rectangle, mGal, for comparison with the "observed" field shown in Fig. 9) from a 3-D average lower crust density distribution (dashed lines, 10^3 kg m^{-3}).

crustal heterogeneities, $\Delta g_{lwcr} = \Delta g_{cr} - \Delta g_{upcr}$ (Fig. 9). These anomalies were then fitted by trial and error to a model 3-D density distribution in 15 km depth to Moho layer. The final version of this density model and its calculated effect are shown in Fig. 10. There are three dense bodies in the lower crust (average density 2960 kg m^{-3}): (1) areas of granulitic consolidation in the PD and southern part of the RTD; (2) the OMIB; and (3) the Chernigov segment of the Dnieper Graben. Lower crust of reduced density (down to $\rho \approx 2850$ kg m^{-3}) is inferred for the region including the northern part of the KP and a major part of the PT.

The total effect of the model Δg_{tot}, obtained by summing the effects of all the model layers, $\Delta g_{tot} = \Delta g_{sed} + \Delta g_{upcr} + \Delta g_{lwcr}$, is shown in Fig. 11. There is quite good agreement between Δg_{tot} (Fig. 11) and g_{obs} (Fig. 3). The misfit $\Delta g_{resfn} = \Delta g_{obs} - \Delta g_{tot}$ is in the range of ±10 mGal, indicating an excellent model fit, especially given that the observed field has amplitudes ranging from −60 to +80 mGal. Regional modelling also substantiates a role for the deep N–S

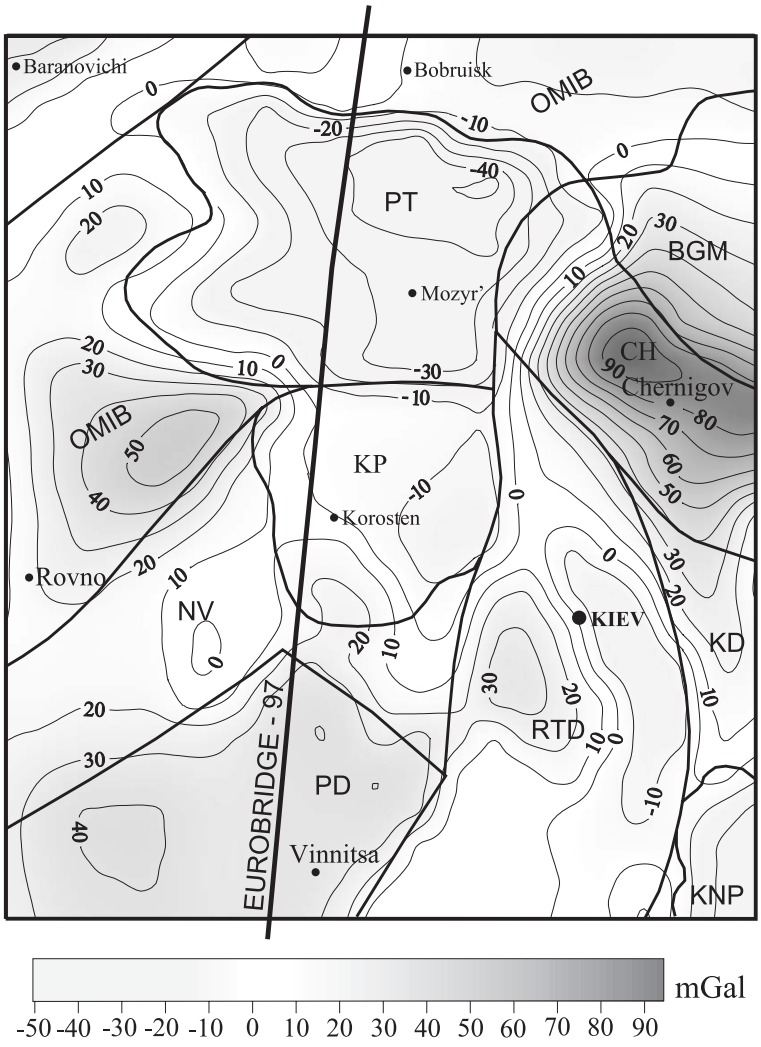

Fig. 11. Total effect of the 3-D density model for the crust of EB'97 area (mGal) obtained by summing the effects of sediments (Fig. 5), upper crust (Fig. 6b), and lower crust (Fig. 10).

trending Odessa–Gomel tectonic zone, which separates granulite–basic (to the west) and greenstone segments of the Archean protocrust (Bogdanova, 1984). Recently obtained age determination data (Stepanyuk et al., 1998) support the idea that this zone is a suture between mainly Archean (PD and southern part of the RTD) and Proterozoic crustal segments.

4. Gravity modelling along the EUROBRIDGE-97 profile

Velocity models determined along the EUROBRIDGE-97 (EB-97) refraction/wide-angle reflection seismic profile (Thybo et al., 2003) provide a basis for 2-D gravity modelling along this profile, which transects the area of the 3-D gravity analysis. The initial V_p velocity model used as a starting point for the gravity modelling is shown in terms of isovelocity contours in Fig. 12. The three main geological units mappable at the basement surface can be distinguished: (1) the OMIB with the PT, 0–210 km; (2) the KP, 210–300 km; and (3) the PD, 300–520 km. Deeper than about 12 km there is no evident correlation of near-surface geological structure. At this depth, four segments with boundaries at approximately 140, 300, and 410 km can be seen. A V_s model as well as V_p/V_s ratios, suggests a similar division (Thybo et al., 2003). The most pronounced feature of the middle and lower crust is in the range of 140–300 km, which includes the southern part of the OMIB and major part of the KP. In this the $V_p = 6.6$ km s^{-1} contour rises to a depth of about 13 km at 205 km (Fig. 12), while at the end of the profile (500 km) it deepens to 26 km. The $V_p = 6.8$ km s^{-1} contour, located at a depth of about 30 km at 205 km, deepens to 40 km at the beginning of the profile. A fundamental change in crustal structure in the depth range 12–15 km is consistent with 3-D residual gravity analysis presented above (which inferred crustal heterogeneities in the upper crust). A 5-km-thick high-velocity lens ($V_p = 7.5$–7.6 km s^{-1}) of complex configuration, distinguished in the lower crust (140–410 km), most likely represents a crust–mantle transition zone. A major upper mantle reflector, below the OMIB/PT dipping southward under the KP was also inferred from the seismic data (Fig. 12).

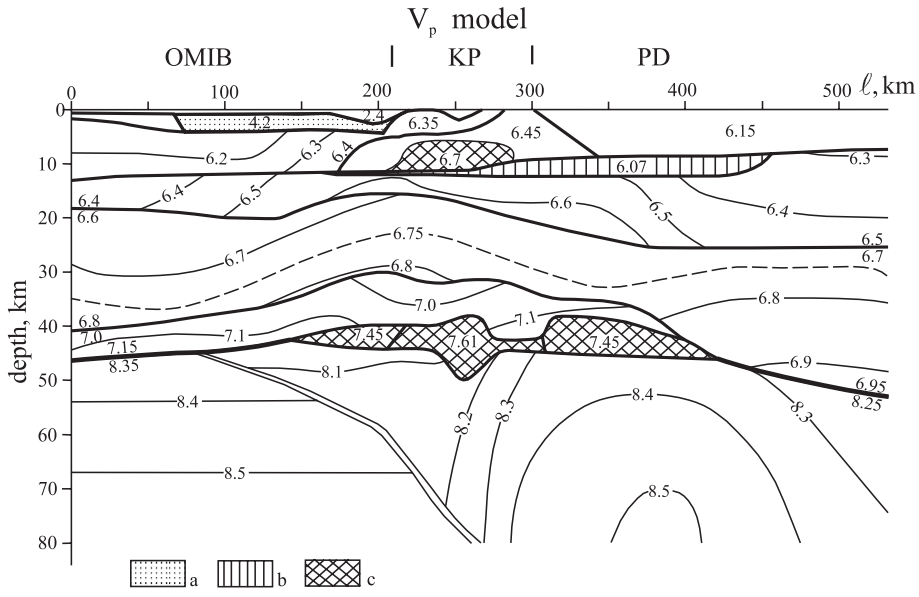

Fig. 12. P-wave velocity modes along the EB'97 profile (Thybo et al., 2003); contour values are in km s^{-1}. Patterned zones are a—low-velocity sediments of the Pripyat Trough; b—inversion zone at the base of the upper crust; and c—high-velocity zones.

The V_p model (Fig. 12) was converted into its density equivalent, shown in Fig. 13, using the relationship $\rho = 320\,(V_p) + 730$ kg m^{-3}. The gravity effect calculated directly from the converted density model differs markedly from the observed field (Fig. 13), though the pattern is similar over the PT. Elsewhere, trends as well as amplitudes are very different: the calculated curve, in contrast to the observed, shows a gravity high over the KP and a low on the PD.

To eliminate such a strong disagreement between the seismic interpretation and its implications for the gravity field, we were obliged to modify the initial velocity model (Fig. 12) using an interpretation of the EB'97 data made at the Institute of Geophysics in Kiev (Ilchenko, 2002) in combination with a reinterpretation of DSS profiles II and VI (Ilchenko and Bukharev, 2001) where they intersect with EB'97. In particular, for the DSS profile II, where it crosses the KP, indicates an interlayering of high (6.5 km s^{-1}) and low (5.8–6.0 km s^{-1}) velocity bodies (interpreted as anorthosites and rapakivi granites) that allowed the base of KP to be determined as 16 km in its southern part (Trypolsky et al., 2000; Ilchenko and Bukharev, 2001). The calculated gravity curve of this model (Fig. 14) is better than the initial one, although in some ways it remains similar. It is improved over the OMIB and the divergence in the interval 230−515 km have been somewhat reduced.

The divergence of the calculated and observed gravity fields indicates a significant deviation of the ρ/V_p relationship from the standard one that was used. This is supported by the data tabulated in Table 1 and plotted in Fig. 2: granitoids of the VD and intrusive

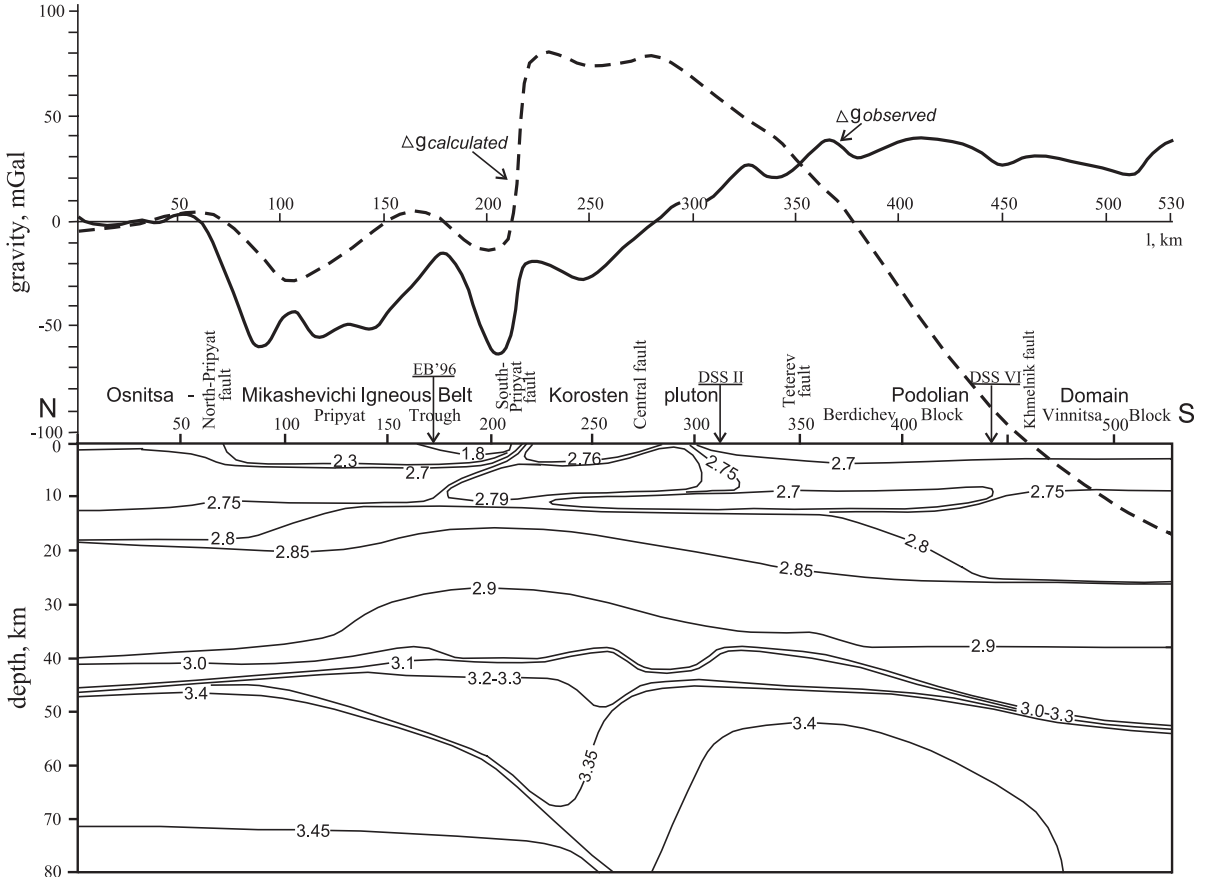

Fig. 13. Initial density model along the EB'97 profile, obtained directly from the velocity model in Fig. 12, and its calculated gravity effect compared to observed gravity. Contour values are in 10^3 kg m^{-3}.

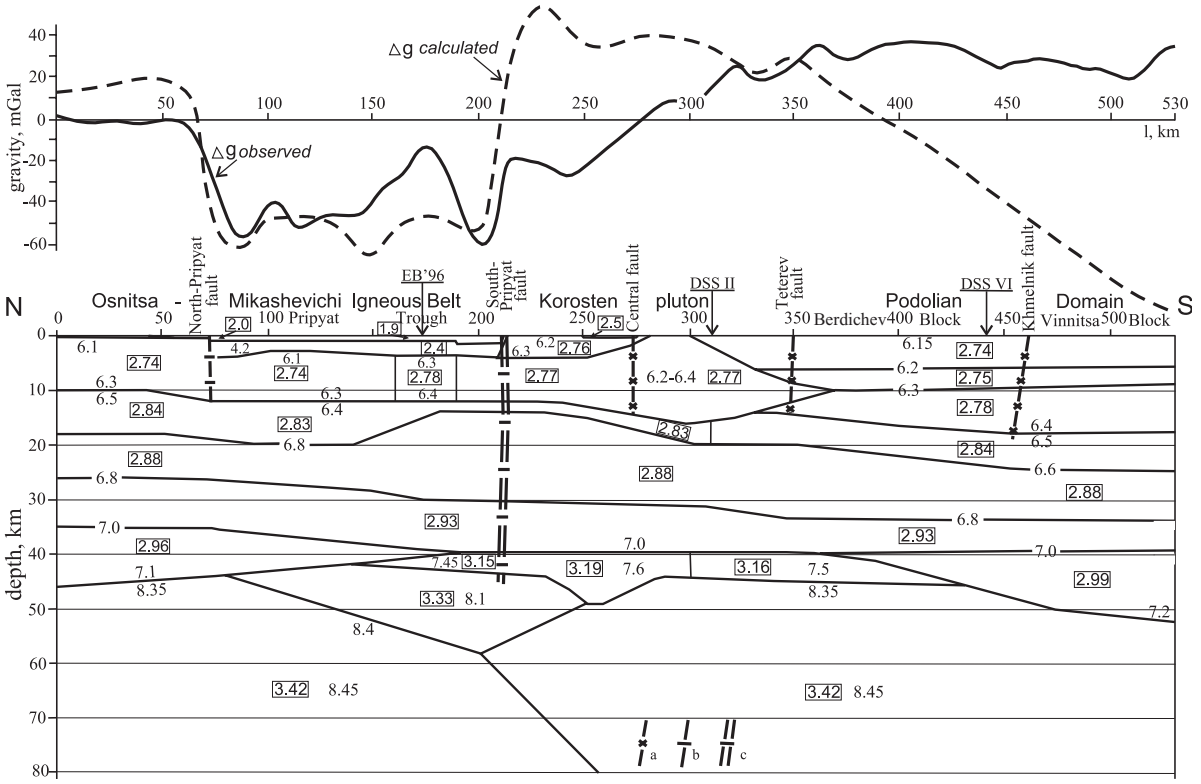

Fig. 14. Generalised velocity/density model of the EB'97 profile (km s^{-1} and 10^3 kg m^{-3}, respectively, the latter in rectangles) constructed from the seismic model (Thybo et al., 2003), modified according to Ilchenko, 2002, and new interpretations of DSS profiles II and VI (Ilchenko and Bukharev, 2001). Deep faults: a—diagonal; b—west–east orientated; c—west–east orientated penetrating to the mantle.

rocks of the KP have lower densities (2630–2650 kg m^{-3}) in comparison with the standard whereas mafic granulites of the PD are characterised by higher densities. Fig. 15 shows a model in which these density–velocity perturbations have been incorporated. Additionally, its upper part was modified according to the 3-D model (see Section 3.3) and the geological setting of the Ukrainian Shield in the vicinity of EB'97, in particular, occurrences of mafic rocks and enderbites at intervals 310–320 and 350–370 km.

The upper part of the density model in the area of KP has been significantly changed compared with initial model. South of the Central fault (270 km) the pluton is composed of interlayered rapakivi granites (40%) and anorthosites (60%) that result in an average density of 2720 kg m^{-3}, correlating with an average V_p of 6.45 km s^{-1} in this part of the pluton. Its northern part comprises predominantly rapakivi granites of ρ=2630–2650 kg m^{-3}. It should be noted that the gravity effect of these rapakivi granites in our 3-D model explains the residual field Δg_{res} low over the northern part of the KP (see Fig. 6a). In the velocity cross-section (Fig. 12), a high-velocity domain (V_p as high as 6.7 km s^{-1}) has been obtained in the depth interval 5–10 km. This apparent contradiction of a high-velocity domain coinciding with a gravity low in the KP can be explained, in our opinion, by the combined effect of two factors: (1) perturbation from the standard ρ/V_p function in intrusive rocks (see Fig. 2); and (2) quasianisotropy. The latter can occur in a layered high- and low-velocity medium when the recorded and modelled seismic wave velocities are controlled by the high-velocity layers resulting in a higher modelled velocity compared with the true bulk velocity of the massif. The

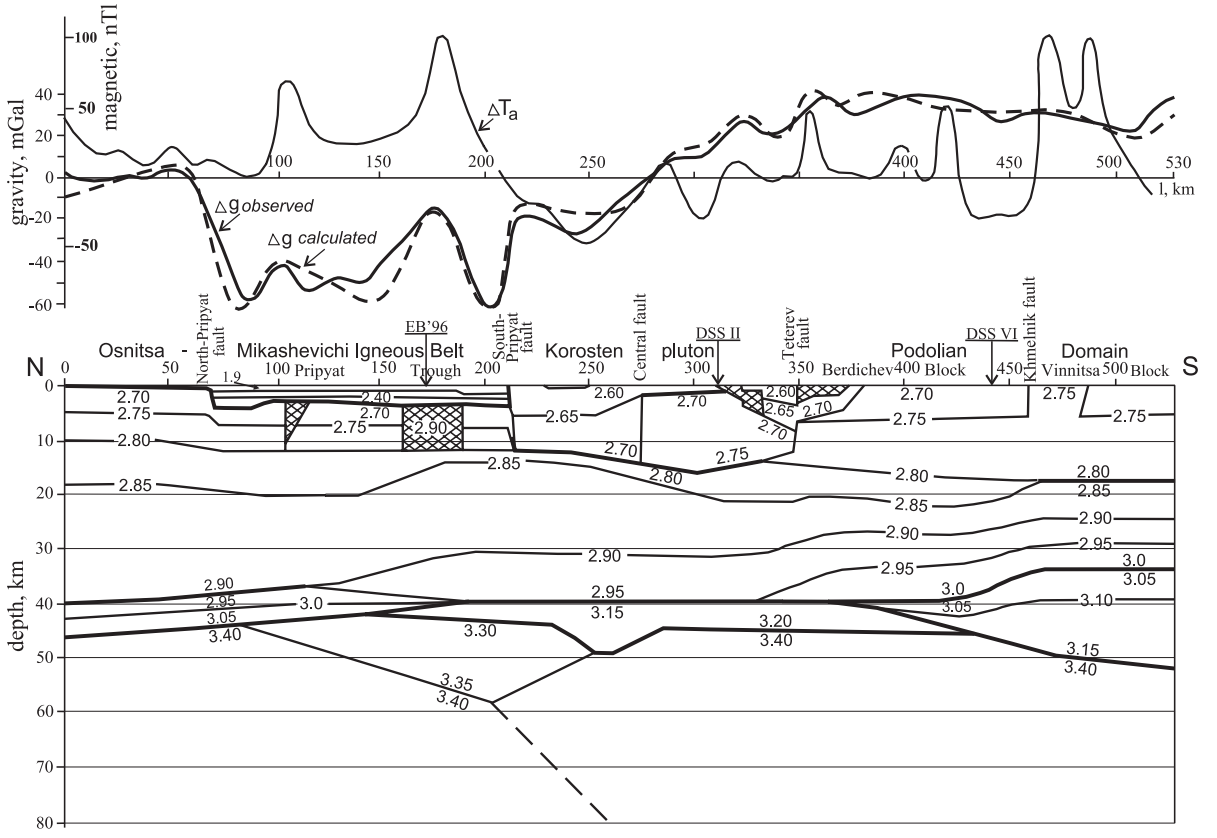

Fig. 15. Density model along the EB'97 profile (10^3 kg m^{-3}) based on the generalised velocity model shown in Fig. 14 using specified velocity/density functions (Fig. 2). Hatched areas indicate high-density bodies in the upper crust associated with mafic intrusion.

density model was accordingly revised, by trial and error giving the cross-section seen in Fig. 15, in which misfits with the observed field lie within the limits of ±10 mGal.

5. Interpretation of the density models and discussion

Gravity modelling of the EB'97 profile has revealed large differences in crustal structure along the profile and has confirmed the division of the crust on three main domains. These are (from the north to the south) the Osnitsa–Mikashevichi Igneous Belt (OMIB) with the superimposed Pripyat Trough (PT) and two domains in the Ukrainian Shield–Volhyn, being the Korosten Pluton (KP) and Podolian Domain (PD). The structural distinctions between domains, caused mainly by their different Precambrian histories, are more evident in the density model than in the corresponding velocity model. In particular, this is seen in the case of the PD, where the deep structure of this Archean granulitic core is not expressed in the velocity model as strikingly as in the density model.

V_p/V_s ratios (Thybo et al., 2003), which can be related to SiO_2 content (Khalevin, 1980), were also used in the interpretation, according to a non-linear relationship (Krilov et al., 1990). The resulting SiO_2 content distribution along EB'97 is shown in Fig. 16. Three categories of crustal compositions are distinguished: felsic, with SiO_2>65% (upper crust); intermediate, with SiO_2 content 55–65% (middle crust); and mafic, with SiO_2<55% (lower crust). The EB'97 crustal structure inferred from the gravity modelling basically corresponds to the block-layered model of

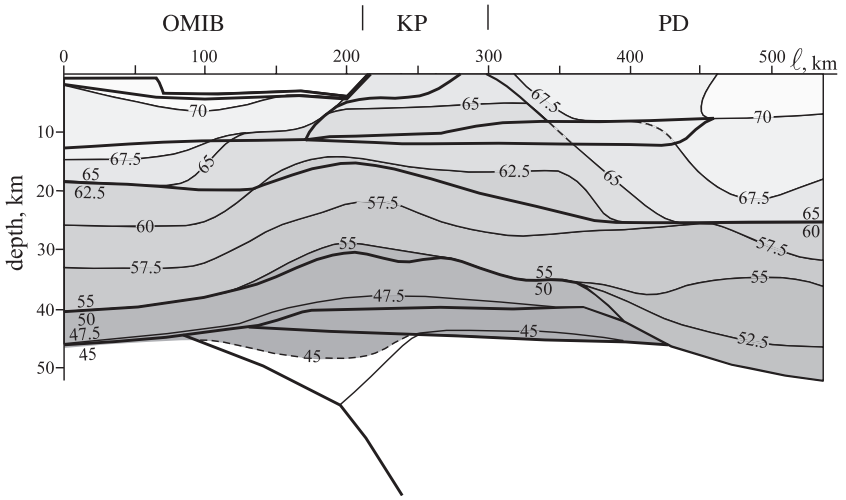

Fig. 16. SiO_2 content (%) in the crust on the EB'97 profile, estimated from V_p/V_s ratios (Thybo et al., 2003) using the relation of Krilov et al. (1990).

Pavlenkova (1988): a 10–15-km-thick heterogeneous upper crust with V_p=5.8–6.4 km s^{-1} consisting of blocks and corresponding to a brittle layer in which shear zones, thrusts, and normal faults are formed (cf. Fig. 14). At greater depths, ductile deformation prevails, leading to a predominance of layered structures and flattening of faults.

Fig. 17 is a composite diagram showing velocities, densities, and inferred silica content along EB'97 and including an interpretation of these in terms of rock type. Granodioritic and dioritic rocks are widespread in the 2.0–1.95 Ga old OMIB, which marks the suture between Fennoscandia and Sarmatia (Gorbatschev and Bogdanova, 1993; Bogdanova and Gorbatchev, 1998). However, in the granodioritic (V_p = 6.1–6.3 km s^{-1}, ρ = 2740–2750 kg m^{-3}, $SiO_2 \approx$ 68–70%) upper crust, there are two anomalous bodies beneath the PT. These have ρ = 2900 kg m^{-3} and correspond to local gravity and magnetic anomalies (110 km and 170–190 km; Fig. 15). The southern body, located in the vicinity of the South Pripyat Fault (SPF), coincides with a residual gravity high connecting the Osnitsa and Chernigov highs (Fig. 6a). This anomaly is interpreted to be caused by mafic rocks intruded into the crust during the Late Devonian rifting that formed the PT. The middle crust (V_p=6.5–6.8 km s^{-1}, $\rho \approx$ 2880 kg m^{-3}, $SiO_2 \approx$ 65–57%) is, probably, represented by rocks close to dioritic composition and rocks of amphibolitic, partly granulitic metamorphic grade. The thin lower crust of the OMIB (V_p = 7.0–7.1 km s^{-1}, ρ = 2930–3000 kg m^{-3}, $SiO_2 \approx$ 48%) has a granulite–basitic composition and thickness increasing from 7 km in the north to 12 km in the south, in the vicinity of SPF. According to seismic data (Juhlin et al., 1996), the SPF is listric dipping northward under the PT and flattening at the top of the lower crust at a depth of about 30 km.

The crustal structure of the PD can be explained by its affinity with Archean crust (3.4–3.7 Ga) and widespread development of rocks of granulitic metamorphic grade. The inferred deviation from the standard velocity/density relation may be one consequence of this, manifested as a general density increase within all crustal layers (cf. Fig. 15), along with a decrease of V_p/V_s ratio and implicit decrease of SiO_2 content. This phenomenon needs further investigation. The upper crust (V_p = 6.1–6.4 km s^{-1}, ρ = 2740–2780 kg m^{-3}) is represented at the surface by Berdichev granites, which give way at depth to charnockites and enderbites. Its thickness, approximately 18 km, has been estimated on the basis of the 6.4 km s^{-1} velocity contour and corresponding zone of silica content ≥68%. It should be noted that these results are not consistent with the idea, based on the DSS profile VI (Chekunov, 1976), that the top of the middle crustal layer in the PD is uplifted to a depth of

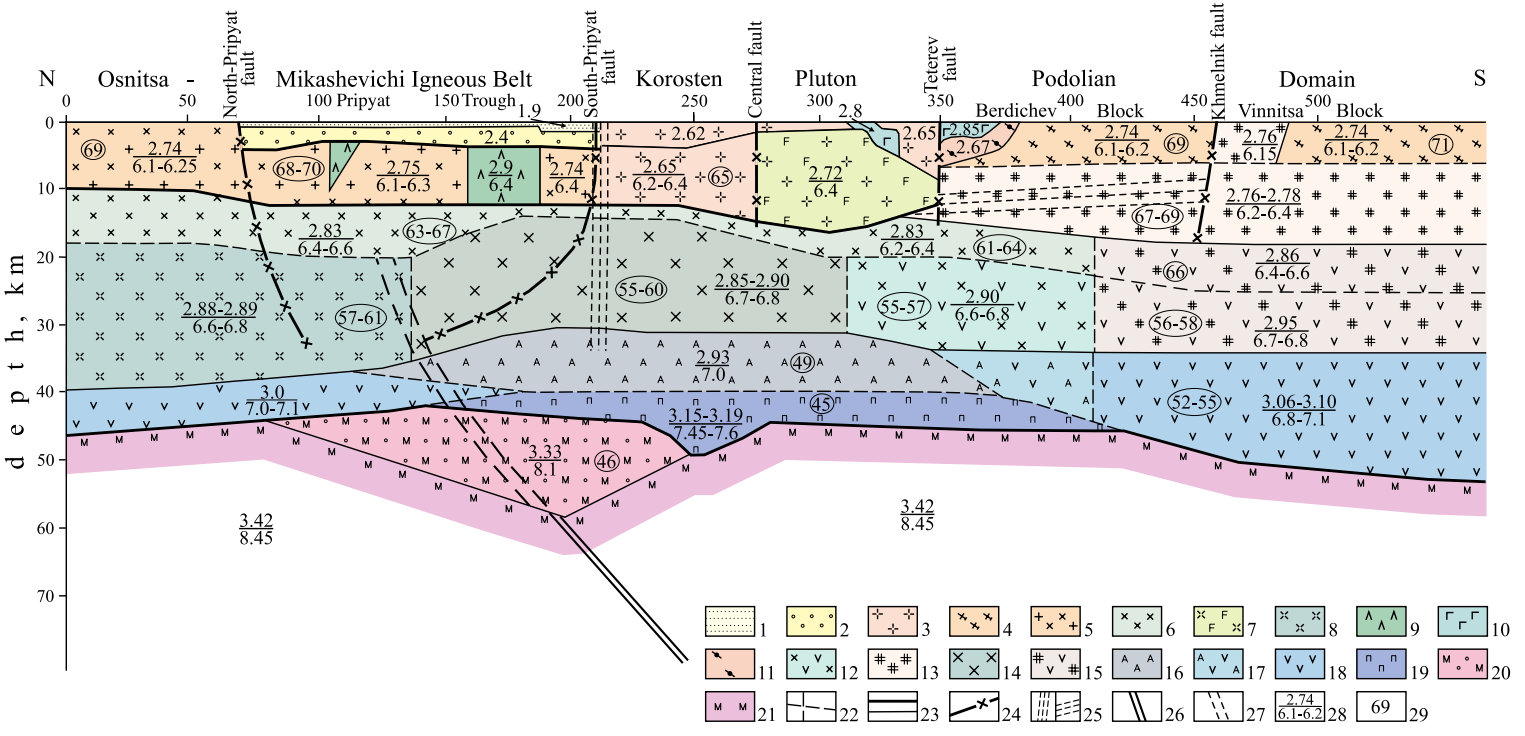

Fig. 17. Velocity-density model along the EB'97 profile with a compositional interpretation of crustal layers. 1—Unconsolidated sediments of the PT; 2—compacted sediments of the PT; 3—rapakivi granites; 4—Berdichev granites; 5—granites and granodiorites (of Osnitsa complex); 6—granodiorites; 7—interlayering of anorthosites and rapakivi granites; 8—diorites; 9—basic rocks; 10—gabbro, gabbro–monzonites; 11—biotite gneisses; 12—diorites and enderbites; 13—charnockites and enderbites; 14—middle crust of mainly dioritic composition; 15—enderbites and mafic granulites; 16—amphibolites; 17—amphibolites and granulites; 18—mafic granulites; 19—peridotites; 20—upper mantle of decreased density; 21—upper mantle; 22—boundaries between layers and blocks of different properties; 23—boundaries between crustal stages (thick lines) and main crustal layers (thin lines); 24—faults exposed at the surface; 25—probable zones of tectonic disruption; 26—seismic reflector in the upper mantle; 27—southern edge of the suture zone between Fennoscandia and Sarmatia according to Bogdanova and Gorbatchev (1998); 28—modelled values of density in 10^3 kg m^{-3} and V_p in km s^{-1}; 29—SiO_2 content (%) inferred from V_p/V_s ratios.

about 8 km. The middle crust in the PD (18 km in thickness, $V_p = 6.4–6.8$ km s^{-1}, $\rho = 2860–2950$ kg m^{-3}) is thought to be composed of enderbites, replaced in its lower part by granulites.

The crustal thickness in the PD, with the Moho deepening to 50 km and more, is the greatest observed along the profile. Thick lower crust (about 17 km with $V_p = 6.8–7.1$ km s^{-1}, $\rho = 3060–3100$ kg m^{-3} and $SiO_2 \approx 52–55\%$) may comprise mainly granulites and, at its base, possibly rocks with ultramafic composition. A body is inferred at depth below the boundary between the Podolian and Volhyn domains (in the distance interval 310–410 km in the middle and lower crust), which according to its parameters (V_p=6.6–6.8 km s^{-1}, $\rho \approx 2900$ kg m^{-3} and $SiO_2 \approx 55–58\%$) may be intermediate in composition.

Crustal features in the Volhyn Domain are characterised, above all, by the presence of the KP, which displays a complex character. Its northern edge is limited by the SPF. Upper crustal composition in the area of the KP ($V_p = 6.2–6.4$ km s^{-1}, $\rho = 2620–2720$ kg m^{-3}, $SiO_2 \approx 65\%$) relates to interlayered intrusive rocks, these being rapakivi granites and anorthosites. The northern part of the pluton, separated from its southern segment by the Central Fault (Fig. 17), is considered to be composed of rapakivi granites, whereas the southern part of the pluton (in the section of the EB'97 profile) is thought to be formed by interlayering of anorthosites and granites with an average density 2720 kg m^{-3}. The KP is surrounded by sedimentary and volcanic rocks of Teterev series and granitoids of Zhitomir complex.

The lower crust below the KP and southern part of the PT has a complicated structure. A layer with $V_p \approx 7.0$ km s^{-1} ($SiO_2 \approx 49\%$) has been distinguished at a depth of 30–40 km. The modelled density values (2930 kg m^{-3}) seem to be too low to represent mafic granulites, so these are considered unlikely to be the major constituent of the crust. Most likely this layer comprises high-temperature amphibolite facies rocks transitional to rocks of granulite facies. Immediately underlying this layer is a high-velocity (density) lens with $V_p = 7.5–7.6$ km s^{-1} and $\rho = 3150–3190$ kg m^{-3}, representing, probably, a lower crust to upper mantle transition zone. In the model (Figs. 15 and 17), this lens, based on velocities, is attributed to a mafic to ultramafic lower crust, a conclusion supported by a silica content estimation of about 45%.

A seismic reflector is clearly seen deepening southward under the KP in the upper mantle below the SPF. This feature is likely related to the suture zone between Fennoscandia and Sarmatia, traced in the upper mantle to the depth of at least 80 km (Thybo et al., 2003). A subcrustal block of decreased velocity compared to adjacent upper mantle (8.10 km s^{-1} versus 8.35 km s^{-1}) lies above this reflector. A body with correspondingly reduced density (3330 kg m^{-3}) has been inferred up to 58 km depth under the PT and northern part of the KP.

Our interpretation of the gravity modelling results in the area of KP is generally consistent with those of similar igneous massifs in other regions (Velikoslavinsky et al., 1978; Emslie, 1978; Korja and Heikkinen, 1995; Elo and Korja, 1993; Puura and Floeden, 1998) and with the hypothesis of complex rapakivi–anorthosite massif formation as a result of partial melting in the upper mantle–lower crust (Eklund and Lindberg, 1992; Rämö, 1991; Emslie et al., 1994). With respect to the KP this hypothesis implies the following. At about 1.9 Ga, soon after (or almost coincident with) the formation of the OMIB, a partial melt chamber (related to the underthrusting of terranes in the lower crust and upper mantle according to Duchene et al., 1998) formed in the subcrustal mantle (Fig. 17). The inferred low-velocity/density body ($V_p = 8.10$ km s^{-1} and $\rho = 3330$ kg m^{-3}) is interpreted as a remnant of such a magma chamber, in the form of lens immediately below the Moho underlying the OMIB and KP (in the interval 70–220 km). Basaltic magmas fanned out laterally to generate a magma pond at the base of the crust.

Thus, the formation of the KP is strongly linked to the development of the southeastern limits of the OMIB. There is also a link between the KP and the SPF—the southern border of the PT, which formed only in the Late Palaeozoic as a result of intracratonic rifting. The Palaeozoic rift system, which includes the Dnieper–Donets Basin to the southeast (cf. Stephenson et al., 2001), separates the Precambrian Ukrainian Shield (to the south) and the Voronezh Massif (to the north). It has been argued that the rift trend inherits a very long-lived zone of extension, traced from east of the Caspian Sea to Poland—the so-called Sarmato–Turanian lineament (Aizberg et al., 1971; cf. Yegorova et al., 2004). The KP possibly lies at the inter-

section, therefore, of two diagonal tectonic zones: the generally northwest orientated Sarmato–Turanian lineament and the northeasterly trending suture zone between Fennoscandia and Sarmatia, marked by the Palaeoproterozoic OMIB.

Thus, the link between the inferred fossil magma chamber and the upper mantle reflector dipping southward under the KP is noteworthy. This reflector is primarily associated with the complex subduction/collisional suture between (Palaeoproterozoic) Fennoscandia and (mostly Archean) Sarmatia (Bogdanova and Gorbatchev, 1998; Thybo et al., 2003). Several authors (Gower and Tucker, 1994; Scoates and Chamberlain, 1995; Funk et al., 2000) have noted that anorthosite complexes are often located near the boundaries of Archean cratons and Palaeoproperozoic orogens. Scoates and Chamberlain (1995) proposed that inherited crustal structure provided zones of lithospheric weakness that facilitated the generation and ascent of anorthositic magmas.

The emplacement of rapakivi–anorthosite massifs in the Ukrainian and Baltic shields (i.e. Sarmatia and Fennoscandia, respectively) occurred during the subplatform stage of evolution, during which mature continental crust (comprising an assembly of different terranes) responds to regional tectonic stresses (either compressional or extensional depending on changing plate boundary conditions) along pre-existing fault systems. Once a partial melt chamber was generated in the upper mantle beneath the OMIB, granitic magmatism would have occurred as a result of anatexis in the lower crust. The granitic magmas, rising to the surface along a system of reactivated faults (including the proto-SPF), led to the formation of rapakivi granite massifs. Large volumes of anorthositic melts were developed at a later stage, when residual mafic granulites (after production of granitic magmas) were assimilated by mantle-derived basaltic melts, forming large magma chambers in the uppermost mantle (e.g. the high-velocity/density lens in the lower crust discussed above). Such an interpretation is also consistent with seismic data from the Åland Massif (Lefmann and Thybo, 1998). Subsequently, the anorthositic magmas ponded in the lower crust were emplaced as anorthositic plutons (massifs) at upper to midcrustal levels. A similar scenario for the KP was proposed by Ilchenko and Bukharev (2001), although these authors considered the rapakivi granites to have formed in situ as a result of granitisation of pre-existing parent rocks. However, this appears to be ruled out by very uniform composition of rapakivi granites observed world-wide.

The parent magmas of the anorthosite bodies in the central and southern parts of the massif—Volodarsk–Volynsk and Chepovichi—were intruded along diagonal faults in the central part of the pluton according to Gintov et al. (1974). Conduits for acid magmas that formed the large rapakivi granite massifs in the northern part of the KP, were generally controlled by the E–W orientated SPF. That faults lying parallel to the (much younger) Pripyat–Dnieper–Donets Basin played an important role during the emplacement of large rapakivi–anorthosite massifs in the Ukrainian Shield, including the KP and the similar Korsun–Novomirgorod pluton was suggested earlier by Sollogub et al. (1981) and Chekunov (1994).

Indirect proof that the SPF was a magma channel for the KP is the linear Ovruch Depression (see Fig. 1), filled with sandstones, overlying the KP and parallel to the SPF. It is assumed to have originated as a result of subsidence during post-emplacement cooling and may indicate the locus of maximum thickness of rapakivi granites and/or the location of the acid magma source conduit. The Jotnian sandstone basin overlying the rapakivi Åland Massif (Baltic Shield) may provide an analogue for the Ovruch Depression in terms of its structure and mechanism of formation (Lefmann and Thybo, 1998).

The density/velocity models presented in this work have so far been interpreted primarily in terms of the petrology and bulk composition of the crust. However, it is known from superdeep well data that stable Precambrian cratons can be significantly disturbed as a result of large-scale faulting and/or shearing. Large fault/shear zones can lead to seismic attenuation (Kozlenko, 2002). The subhorizontal low-velocity lens at the base of upper crust (in the interval 300–400 km and depth ~12 km; V_p=6.07 km s^{-1}; Fig. 12) can possibly be explained in such a way. It is perhaps noteworthy that the same area is one of with indications of recent tectonic activity, thought to be one of most active areas within the East European Platform (Golizgra and Logvin, 1998). The possible geody-

namic implications of this correlation deserve further special consideration.

6. Summary and conclusions

The results of the gravity modelling carried out in the region of the EUROBRIDGE-97 seismic profile can be summarised as follows.

(1) A 3-D regional density model of the Earth's crust shows that density heterogeneities within the upper crust (shallower than 15 km) can explain the main features of the observed gravity field. The study region is characterised by a large variation of density in upper crustal units (from 3000 kg m^{-3} in the Chernigov block of the Pripyat–Dnieper–Donets Basin to 2650 kg m^{-3} in the Korosten Pluton). Density heterogeneities deeper than 15 km are influenced by Moho topography. Modelling of densities in the middle and lower crust requires, in accordance with the principle of isostasy, denser crustal blocks where the Moho is deeper and less dense crust where the Moho is shallower, such as below the Korosten Pluton and a major part of the Pripyat Trough.

(2) The presence of the N–S orientated Odessa–Gomel tectonic zone, dividing the crust of the study area onto two regions—mainly of Archean age to the west (Ros–Tikich and Podolian domains) and of Proterozoic age to the east (Kirovograd Domain)—has been substantiated by the 3-D modelling.

(3) Profound contradiction between the velocity structure and observed gravity field revealed by gravity modelling along the EUROBRIDGE-97 seismic profile is explained by a perturbed velocity/density relationship for the Podolian Domain, where Archean mafic granulites are exposed on the surface, and in the rapakivi–anorthosite Korosten Pluton, where the effects of quasi-anisotropy are thought to play a role.

(4) The best-fitting gravity model for EUROBRIDGE-97 profile, taking into account all other available geological and geophysical data, supports the presence of three main crustal domains—the Osnitsa–Mikashevichi Igneous Belt (with the superimposed Pripyat Trough), the Korosten Pluton of the Volhyn Domain, and the Podolian Domain—forming an upper crust of heterogeneous block structure. A link between surface geology and the inferred structure and composition of the middle and lower crust is not apparent. Subhorizontal layered structures prevail. The most complicated lower crustal structure and the shallowest Moho lie below the Korosten Pluton. The greatest crustal thickness (more than 50 km) is found, according to the seismic data, in the Podolian Domain.

(5) The status of the Podolian Domain as an Archean granulitic core is supported by a density increase in all crustal layers that coincides with a downward bending of V_p contours (i.e. relative velocity reduction). Characteristics typical for the upper crust—silica content up to 65% and $V_p \leq 6.4$ km s^{-1}—have been obtained for the uppermost layer of the Podolian Domain crust, which is as thick as 20 km.

(6) The EUROBRIDGE-97 data reveal that the rapakivi–anorthosite Korosten Pluton comprises a body that is 12–17 km thick and divided by the Central Fault into two parts. The two segments are characterised by differing amounts of granitic component. The complex crustal structure of the Korosten Pluton can be related to processes involved in its origin and emplacement, particularly in the lower crust and in a lower crust–upper mantle transition zone. In general, the inferred structure can be satisfactorily explained by a model of rapakivi–anorthosite massifs formation involving the development of partial melt magma chambers in the upper mantle–lower crust.

(7) The Korosten Pluton is located at the intersection of two diagonal tectonic zones, an Archean-aged NW–SE trending regional fault zone and a younger, Palaeoproterozoic, SW–NE trending igneous belt. An important role for proto-South-Pripyat Fault, repeatedly activated during Archean–Palaeozoic times, has been ascertained. In the Late Proterozoic ($\approx$2.0 Ga) it formed the southeastern boundary of the Osnitsa–Mikashevichi Igneous Belt, which is considered to be part of the suture zone between the (Palaeoprotcrozoic) Fennoscandian and (mostly Archean) Sarmatia units of the East European Craton. Subsequently, at a subplatform stage of the crustal evolution, the South Pripyat Fault was reactivated and likely was a conduit for magmas forming the Korosten Pluton, the deep sources of which were located in the upper mantle–lower crust. In Late Palaeozoic times, the South Pripyat Fault was reactivated again during rifting that led to the formation of the Pripyat Trough. In contrast to the Dnieper–Donets Basin, where the crust was

heavily intruded by mafic magmas during rifting along the rift axis, intrusion of mafic rocks in the Pripyat Trough occurred mainly along the southern flank of the basin and was not so voluminous.

(8) Gravity modelling, carried out in the framework of the excellent EUROBRIDGE-97 seismic data, provides significant additional information for understanding the structure, composition, and responsible endogenic lithospheric processes in the study area. The present results have also elucidated the main problems in the area requiring further investigation. A key unresolved problem relates to the change of structural style in the middle and lower crust compared to the upper crust.

Acknowledgements

The research described in this paper has been carried out in the framework of the EUROBRIDGE project of the European Science Foundation research programme EUROPROBE. Our appreciation goes to the referees—Dr. M.D. Thomas (Geological Survey of Canada), Dr. H. de Boorder (Utrecht University, Netherlands), Prof. G.I. Karataev (Institute of Geology and Geophysics, Minsk, Belarus)—all of whom made valuable recommendations for improving the previous version of the manuscript. We thank R.A. Stephenson for the fruitful discussions and his help in editing the English. M.V. Kozlenko (Institute of Geophysics, Kiev) helped in preparing the figures.

References

Aizberg, R.E., Garetskiy, R.G., Sinichka, A.M., 1971. Sarmato–Turanian lineament of the Earth's crust. In: Peive, A.V. (Ed.), Problems of Theoretical and Regional Tectonics. Nauka, Moscow, pp. 41–51 (in Russian).

Bogdanova, S.V., 1984. Tectonics of the basement of East European platform. Tectonic Investigations of the Western Part of the East European Platform. Nauka i Tehnika, Minsk, pp. 16–28 (in Russian).

Bogdanova, S.V., Gorbatchev, R., 1998. EUROBRIDGE-1998: results and outlooks. Geophys. J. Kiev. 20 (4), 60–63.

Bogdanova, S., Pashkevich, I., Byryanov, V., Makarenko, I., Orlyuk, M., Skobelev, V., Starostenko, V., Legostaeva, O., 2004. The 1.8–1.74 Ga gabbro-anorthsite–rapakivi Korosten pluton in the Ukrainian Shield: a 3-D geophysical reconstruction of deep structure. Tectonophysics 381, 5–27 (this volume).

Chekunov, A.V., 1976. The Earth's crust of the Ukrainian Shield and some important points of basement formation of ancient platforms. Dokl. Acad. Sci. Ukr. SSR 10, 893–896 (in Russian).

Chekunov, A.V. (Ed.), 1987. Lithosphere of the Central and Eastern Europe. Geotraverses I, II, V. Naukova Dumka, Kiev, p. 168 (in Russian).

Chekunov, A.V. (Ed.), 1988. Lithosphere of the Central and Eastern Europe. Geotraverses IV, VI, VIII. Naukova Dumka, Kiev, p. 172 (in Russian).

Chekunov, A.V. (Ed.), 1989. Lithosphere of the Central and Eastern Europe. East European platform. Naukova Dumka, Kiev, p. 180 (in Russian).

Chekunov, A.V. (Ed.), 1992. Scheme of deep structure for the lithosphere of southwestern part of East European platform, scale 1:1000000. In: Zaritsky, A.I. (Ed.), Set of Maps "The Geology and Metallogeny of Southwestern Part of East European Platform". Ukrainian State Geological Committee, Kiev.

Chekunov, A.V., 1994. To the geodynamics of the Dnieper–Donets rift syneclise. Geophys. J. Kiev 16 (3), 3–13 (in Russian).

Chirvinskaya, M.V., Sollogub, V.B., 1980. Deep Structure of the Dnieper–Donets Aulacogen from Geophysical Data Naukova Dumka, Kiev. 178 p. (in Russian).

Duchene, J.C., Auwera, J.V., Liégeiois, J.P., Longhi, J., 1998. The crustal tongue melting model: phase diagram constraints on the origin of anorthosites and tectonic setting. Geophys. J. Kiev 20 (4), 70–71.

Dziewonski, A.M., Hales, A.L., Lapwood, E.R., 1975. Parametrical simple Earth models consistent with geophysical data. Phys. Earth Planet. Inter. 10, 12–48.

Eklund, O., Lindberg, B., 1992. Interaction between basaltic melts and their wallrocks in dykes and sills in Aland, southwestern Finland. Geol. Fören. Stockh. Förh. 114, 93–102.

Elo, S., Korja, A., 1993. Geophysical interpretation of the crustal and upper mantle structure in the Wiborg rapakivi granite area, south-eastern Finland. Precambrian Res. 64, 273–288.

Emslie, R.F., 1978. Anorthosite massifs, rapakivi granites and late Proterozoic rifting of North America. Precambrian Res. 7, 61–98.

Emslie, R.F., Hamilton, M.A., Thériault, R.J., 1994. Petrogenesis of a mid-Proterozoic anorthosite–mangerite–charnockite–granite (AMCG) complex: isotopic and chemical evidence from the Nain Plutonic Suite. J. Geol. 102, 539–558.

Gintov, O.B., Patrikyan, R.P., Timoshchenko, A.I., 1974. Korosten complex pluton as a giant circular (ring) structure. J. Geol. Kiev 34 (3), 73–81 (in Russian).

Golizgra, G.Ya., Logvin, V.N., 1998. The interpretation of geophysical fields along the EUROBRIDGE transect: a study of deep structure and dynamics of the Earth's crust formation. Geophys. J. Kiev 20 (4), 80–81.

Gorbatschev, R., Bogdanova, S., 1993. Frontiers in the Baltic shield. Precambrian Res. 64, 3–21.

Gordienko, V.V., 1999. Density Models of the Tectonosphere of the Territory of the Ukraine Intellect, Kiev. 100 pp.

Gower, C.F., Tucker, R.D., 1994. Distribution of pre-1400 Ma crust in the Grenville province: implications for rifting in Laurentia–Baltica during geon 14. Geology 22, 827–830.

Funk, T., Louden, K.E., Reid, I.D., 2000. Wide-angle seismic imaging of a Mesoproterozoic anorthosite complex: the Nain Plutonic Suite in Labrador, Canada. J. Geophys. Res. 105, 25693–25707.

Ilchenko, T.V., 2002. Results of the DSS study along the EUROBRIDGE-97 profile. Geophys. J. Kiev 24 (3), 67–76 (in Russian).

Ilchenko, T.V., Bukharev, V.P., 2001. A velocity model of the earth's crust and upper mantle of the Korosten Pluton (Ukrainian Shield) and its geological interpretation (along the DSS profile Shepetovka–Chernigov). Geophys. J. Kiev 23 (3), 72–82 (in Russian).

Juhlin, C., Stephenson, R.A., Klushin, S., 1996. Reappraisal of deep seismic reflection Profile VIII across the Pripyat Trough. Tectonophysics 268, 99–108.

Khalevin, N.I., 1980. Shear waves in explosive seismology. In: Pavlenkova, N.I. (Ed.), The Study of Lithosphere and Asthenosphere on Long DSS Profiles. IFZ AN USSR, Moscow, pp. 173–198 (in Russian).

Korja, A., Heikkinen, P., 1995. Proterozoic extensional tectonics of the central Fennoscandian Shield: results from the Baltic and Botnian echoes from the lithosphere experiment. Tectonics 14, 504–517.

Kozlenko, V.G., 1986. The basis for construction of regional seismic and gravity models. In: Magnitskij, V.A., Sollogub, V.B., Starostenko, V.I. (Eds.), Studying the Lithosphere by Geophysical Methods. Naukova Dumka, Kiev, pp. 113–122 (in Russian).

Kozlenko, V.G., 1989. Interpretation of density and velocity models for the crust of Dnieper graben. Geophys. J. Kiev 11 (6), 27–40 (in Russian).

Kozlenko, V.G., 2002. Zones of destruction of the Earth's crust shown in the anomalies of wave and gravity fields. Geophys. J. Kiev 24 (3), 67–76 (in Russian).

Krasovsky, S.S., 1981. Reflection of Continental-Type Crustal Dynamics in the Gravity Field. Naukova Dumka, Kiev. 264 pp. (in Russian).

Krasovsky, S.S., Kupreinko, P.Ya., Ponomariova, T.I., Ryabokon', G.V., Krasovsky, A.S., 1998. 3D gravity model of the earth's crust for the north-western part of the Ukrainian Shield. Geophys. J. Kiev 20 (4), 88–91.

Krilov, S.V., Briksin, A.V., Ten, E.N., 1990. Elastic properties of minerals and crystalline rocks for isotropic models. Geol. Geophys. 12, 101–113 (in Russian).

Krutikhovskaya, Z.A., Pashkevich, I.K., Silina, I.M., 1982. Magnetic Model and Structure of the Earth's Crust of the Ukrainian Shield Naukova Dumka, Kiev. 228 pp. (in Russian).

Kulish, E.A., Gorlitsky, B.A., 1989. Petrochemistry of Precambrian Complexes of the Ukrainian and Aldan Shields Naukova Dumka, Kiev. 190 pp. (in Russian).

Lebedev, T.S., Korchin, V.A., Savenko, B.Ya., Shapoval, V.I., Shepel', S.I., 1986. Physical Properties of Mineral Matter in Temperature–Pressure Conditions Naukova Dumka, Kiev. 193 pp. (in Russian).

Lebedev, T.S., Korchin, V.A., Savenko, B.Ya., Shapoval, V.I., Shepel', S.I., Burtnoy, P.A., 1988. Petrophysical Studies at High PT-Conditions and Their Geophysical Applications. Naukova Dumka, Kiev. 244 pp. (in Russian).

Lefmann, A.K.B., Thybo, H., 1998. Seismic evidence for underplating during formation of rapakivi granites around the Aland Islands. Geophys. J. Kiev 20 (4), 93–95.

Orlyuk, M.I., Pashkevich, I.K., 1996. Magnetic model of the Earth's crust for the south-west of the East European platform. Geophys. J. Kiev 15, 839–847 (in Russian).

Orlyuk, M.I., Pashkevich, I.K., 1998. The sources of upper-crustal magnetism in the part of the Ukrainian Shield traversed by EUROBRIDGE profile. Geophys. J. Kiev 20 (4), 98–99.

Pavlenkova, N.I., 1988. The nature of seismic boundaries in the continental lithosphere. Tectonophysics 154, 211–255.

Puura, V., Floeden, T., 1998. The sequence of mafic and felsic magmatism in the 1.65–1.50 Ga Fennoscandian Rapakivi Province. Geophys. J. Kiev 20 (4), 102–105.

Rämö, O.T., 1991. Petrogenesis of the Proterozoic rapakivi granites and related basic rocks of south-eastern Fennoscandia: Nd and Pb isotopic and general geochemical constraints. Geol. Surv. Finl., Bull. 355, 161.

Scoates, J.S., Chamberlain, K.R., 1995. Baddeleyite (ZrO_2) from anorthositic rocks of the Laramie anorthosite complex, Wyoming: petrologic consequences and U–Pb ages. Am. Mineral. 80, 1317–1327.

Shcherbak, N.P., Skobelev, V.M., Stepanyuk, L.M., 1998. Geological structure and age of the Precambrian Ukrainian Shield along the EUROBRIDGE Transect. Geophys. J. Kiev 20 (4), 105–107.

Sollogub, V.B., Sologub, N.V., Chekunov, A.V., 1981. Sublateral faults in the crystalline substrate of the south of East European platform. Dokl. Acad. Sci. Ukr. SSR, Ser. B 5, 18–22 (in Russian).

Starostenko, V.I., Legostaeva, O.V., 1998. Direct gravity problem for heterogeneous arbitrary truncated prism. Izv. Phys. Solid Earth 12, 31–44 (in Russian).

Starostenko, V.I., Legostaeva, O.V., 1998. Direct gravity problem for arbitrary truncated vertical prism with exponential-dependent on depth density. Dokl. Natl. Acad. Sci. Ukraine 10, 141–147 (in Russian).

Starostenko, V.I., Kozlenko, V.G., Oganesyan, S.M., Shen, E.L., Oganesyan, M.G., Yegorova, T.P., Dyadura, G.V., 1986. 3-D distribution of the density in the crust of Dnieper graben. Geophys. J. Kiev 8 (6), 3–19 (in Russian).

Starostenko, V.I., Matsello, V.V., Aksak, I.N., Kulesh, V.A., Legostaeva, O.V., Yegorova, T.P., 1997. Automation of the computer input of images of geophysical maps and their digital modelling. Geophys. J. Kiev 17, 1–19 (in Russian).

Starostenko, V.I., Buryanov, V., Makarenko, I., Rusakov, O., Stephenson, R., Nikishin, A., Georgiev, G., Gerasimov, M., Dimitriu, R., Legostaeva, O.V., Pchelarov, V., Sava, C., 2004. Topography of the crust-mantle boundary beneath the Black Sea Basin. Tectonophysics 381, 211–233 (this volume).

Stepanyuk, L., Claesson, S., Bibikova, E., Bogdanova, S., 1998. Sm–Nd crustal ages along the EUROBRIDGE Transect in the Western Ukrainian Shield. Geophys. J. Kiev 20 (4), 118–120.

Stephenson, R.A. et al., 1993. Continental rift development in Precambrian and Phanerozoic Europe: EUROPROBE and the Dnieper–Donets rift and Polish Trough basins. Sediment. Geol. 86, 159–175.

Stephenson, R.A., Stovba, S.M., Starostenko, V.I., 2001. Pripyat–Dnieper–Donets Basin: implications for dynamics of rifting and the tectonic history of the northern Peri-Tethyan Platform. In: Ziegler, P.A., Cawazza, W., Robertson, A.H.F., Crasquin-Soleau, S. (Eds.), Peri-Tethys Memoir 6: Peri-Tethyan Rift/Wrench Basins and Passive Margins. Mém. Mus. Natl. Hist. Nat., vol. 186, pp. 369–406.

Thybo, H., Janik, T., Omelchenko, V.D., Grad, M., Garetsky, R.G., Belinsky, A.A., Karataev, G.I., Zlotski, G., Knudsen, U.E., Sand, R., Yliniemi, J., Tiira, T., Luosto, U., Komminaho, K., Giese, R., Guterch, A., Lund, C.-E., Kharitonov, O.M., Ilchenko, T., Lysynchuk, D.V., Skobelev, V.M., Doody, J.J., 2003. Upper lithosperic seismic velocity structure across the Pripyat Trough and Ukrainian Shield along the EUROBRIDGE '97 profile. Tectonophysics 371, 41–79.

Trypolsky, O.A., Kaluznaya, L.T., Omelchenko, V.D., 2000. Features of deep structure of plutons of rapakivi granites and gabbro–anorthosites of the Ukrainian and Baltic shields (by seismic data). Geophys. J. Kiev 22 (6), 121–136 (in Russian).

Velikoslavinsky, D.A., Birkis, A.P., Bogatikov, O.A., Bukharev, V.P., Velikoslavinsky, S.D., Gordienko, L.I., Zinochenko, O.V., Kivisilla, J.J., Kirs, J.E., Kononov, Y.V., Levitsky, Y.F., Niin, M.J., Puura, V.A., Khvorov, M.I., Shustova, L.E., 1978. Anorttosite–rapakivi Suite. East European Craton Nauka, Leningrad. 296 pp. (in Russian).

Yegorova, T.P., 1993. Physical properties of the gabbroides of Korosten Pluton with respect to their ore-perspectivity. Geophys. J. Kiev 15 (4), 54–61.

Yegorova, T.P., Starostenko, V.I., Kozlenko, V.G., Pavlenkova, N.I., 1997. Three-dimensional gravity modelling the European–Mediterranean lithosphere. Geophys. J. Int. 129, 355–367.

Yegorova, T.P., Stephenson, R.A., Kozlenko, V.G., Starostenko, V.I., Legostaeva, O.V., 1999. 3-D gravity analysis of the Dnieper–Donets Basin and Donbas Foldbelt, Ukraine. Tectonophysics 313, 41–58.

Yegorova, T.P., Stephenson, R.A., Kostyuchenko, S.L., Baranova, E.P., Starostenko, V.I., Poppolitov, K.E., 2004. Structure of the lithosphere below the southern margin of the East-European Craton (Ukraine and Russia) from gravity and seismic data. Tectonophysics 381, 81–100 (this volume).